i. Abstract

An autonomous flying platform is one which can hover at a predetermined position whilst remaining stable. Such a vehicle has provided much interest due to the large number of opportunities it creates.

The design and development of such a platform was offered as a fourth year group project to Engineering students at the University of Exeter several years ago. Since then, numerous attempts have been made to fly such a platform, but so far there has been no success. The most significant achievement was made by the 2002 – 2003 group. Using 3 phase motors to drive ducted fans, they were able to achieve high levels of thrust in order to achieve lift. They also designed a control system whereby the platform would try to stabilise itself as a result of a disturbance and demonstrated this in tethered flight.

Between October 2003 and May 2004, the ground work established by the previous group was continued. One of the main issues was that the current design was not able to sustain an onboard power source. This, along with various other aims was covered during the course of the year.

As a group project, the responsibility of the author was primarily concerned with generating a platform power supply and this is covered throughout this report.

ii. Acknowledgments

The author would like to thank the following people whose help was very much appreciated during the course of this project:

- Dr. Martin Jenkins and Dr. Garry Lester for providing the financial and educational support without which this project would not have been possible.
- Mr. Tony Moy from BAE Systems for loaning the project an accurate and precise IMU for use in the control system.
- Mr. Nick Birbeck from IT Services for providing the project with a WebCT storage facility.
- Mr. David Pattison from SAFT for various invaluable information relating to batteries.
- Mr. David Weightman from the Department of Engineering Stores for providing various tools and supplies on requires.
- Dr. Mike Horwood for electronic circuit assistance.
- And finally to my colleagues: Liam Dushynsky, Richard Forder, Richard Holbrook, Rebecca Hughes, Kevin Lowis, Jody Muelaner, Christopher Poczka and Alex Tombling.

iii. Contents

iv. List of Figures

iv. List of Tables

1. Introduction

The concept of a Flying Platform was introduced in the 1940's by Charles Zimmerman [1]. When working for the National Advisory Committee for Aeronautics (N.A.C.A.) Zimmerman prophesised that rotors on top of a vehicle, such as a helicopter, are inherently unstable. He claimed that greater stability could be achieved when controlled from above, similar to the way of riding a bicycle or balancing a surfboard. He coined this term "kinesthetic control". On 17th September 1953, Hiller Helicopters signed a contract with the Office of Naval Research's Naval Sciences Division (ONR) to incorporate Zimmerman's "kinesthetic" theories into developing the a prototype model of a project known as the "Flying Shoes". The first free flight of the unit took place on 27 January 1955, and went in the record books as the first time man had flown a ducted fan vertical take off and landing (VTOL) aircraft. Such a development provided many opportunities, especially for military purposes. The U.S. Army commissioned Hiller Helicopters to construct 2 such vehicles for infantry and reconnaissance use. Several subsequent designs of such manned flying platforms have been developed since, including the De Lackener and Hummingbird Platforms [2].

Figure 1.1: The VZ-1 Pawnee Flying Platform

However, the greatest development challenge comes in the form of Unmanned Aerial Vehicles (UAVs). These may be semi or fully autonomous. In some ways, semi autonomous UAVs are regarded not to be vastly different from manned platforms as the stability control is still achieved by a person. The only difference with a UAV is that this control is by remote transmission from the ground.

Fully autonomous UAVs offer solutions in a wide variety of applications. The military can uses these for improved reconnaissance use as they can be pre-programmed where to go and what to do. Removing any remote radio control means that they can be deployed to areas which may be out of range and, if the situation was hostile, there would be no risk that the platforms would fall into enemy control by interception of the radio signal. Removing the person also opens up a wide range of possibilities. UAVs can be sent on endurance missions for several days or even months without ever needing to return for food or rest [3]. They may also be sent into situations which may currently be considered to compromise human safety.

Other than the military, UAVs have the possibility of being used in other sectors. Such units would be useful for meteorological use for monitoring of different levels of the atmosphere. Other situations such as traffic surveillance, and aerial photography would be a cost effective alternative to hiring or commissioning a manned aircraft [4]. In Italy, the HeliPlat [5] system is currently being developed which aims to act as a relay network for telecommunications. In this situation, UAVs would be an ideal solution as they are considerably cheaper than using satellites and they can be safely brought back to ground for maintenance after remaining in place for possibly months at a time. The successful development of UAVs such as NASA's Solar Powered "Helios" Wing [6] shown in figure 1.2 have made projects such as HeliPlat possible. For use as effective regional transmitters, as depicted in figure 1.3, they need to be at an altitude to high for manned aircraft.

Figure 1.2: NASA's Solar Powered "Helios" Wing during testing [6]

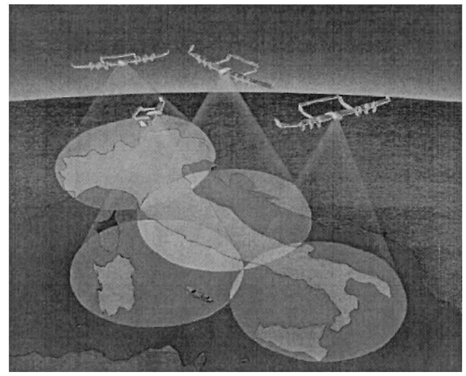

Figure 1.3: The HeliPlat Network [5]

The Design and Development of a Flying Platform has been put forward as a fourth year Engineering project at the University of Exeter by Dr. M.A. Jenkins and Dr. G.A. Lester. For several years the project has been running with several important achievements made by each group. The aim of the exercise is not just to focus on the academics of the problem. Such a project can only be successful through a team effort requiring total commitment from every member. Designing a UAV requires input from a diverse range or Engineering disciplines; a range which one person alone cannot contain. Through organised and effective management, the different academic knowledge and skills of each member can be used to further the progress of such a complex project.

The 2003 – 2004 Flying Platform project saw a variety of new concepts being introduced in light of the achievements made by the previous group. This previous group managed to construct a light weight aluminium structure propelled by 5 ducted electric fans. Stability of this platform was also achieved during tethered flight tests. However, they could not solve the problem of providing enough onboard power to satisfy this stability system. During the course of this year's project, an electric generator was developed powered by an internal combustion engine with the intention that this would provide enough power for stability control and all the onboard electronics. An additional engine was purchased to power a ducted fan and achieve a greater overall thrust. The incorporation of these concepts in the project and their effects is discussed in this report.

2. Review of Previous Achievements

The Design and Development of a Flying Platform has been offered as an annual group project for several years. Previous attempts have examined different propulsion methods with no real continuation from one year to the next.

The 2002 – 2003 group were the first to achieve significant progress through the development of a control system which is successfully interfaced with a new propulsion system. Vertical thrust was provided by 5 WeMoTec Midi fans powered by Plettenberg HP 220/30/A4 SP4 SL brushless 3 phase motors. (Hereafter, these motors will be referred to as HP 220 motors). The speed of the fans could be varied through a Schulze 32.55 speed controller requiring a Direct Current (DC) supply and a Pulse Width Modulated (PWM) control signal. This combination has proved to produce the greatest amount of thrust achieved by any group yet.

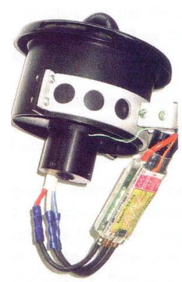

Figure 2.1: Propulsion Ducted Fan using a WeMoTec Midi Fan powered by a Plettenberg HP 220 motor [6]

However, such powerful motors required an electrical source capable of delivering this. As a result, 3 12V Hawker 100Ah Lead Acid batteries were needed each weighing 47kg [7]. Obviously such a source could not be placed on board but if an alternative method was not possible, then this fan and motor combination is inappropriate for the project.

With power supplied by an umbilical to the platform, the control and stability aspect of the problem was tackled. It was found that the response time of the fans with the speed controller would be quick enough to respond to a disturbance input and correct the balance of the platform. Using three electronic gyroscopes mounted at 90° to each other, the change in the angular rotation of the platform could be electronically determined. Three accelerometers also calculated the rate at which the platform moved. Using the outputs from all of these, a control system was developed to correct changes by increasing the thrust from particular fans. This was successfully demonstrated by the group in a tethered flight experiment.

The noticeable achievements made by this previous group during the course of the year would not have been made possible without effective project management and organisation. This was demonstrated by the Chair of the group who successfully maintained the progress of the project by ensuring that all resources were used to the maximum. Regular meetings and the undertaking of tasks concurrently rather than sequentially resulted in the level of progress made.

3. Project Aims

The Project Design Specification (PDS) can be found in Appendix 1. At the beginning of the project, the main objective was to develop on the groundwork established by the previous group resulting in the flight of a stabilised platform by the end of the year. However, owing to continual problems in a variety of areas, this was not accomplished.

It has already been explained that the previous group encountered problems with developing an effective onboard electrical power source [6]. Therefore, a new method needed to be explored. Based on the recommendations of the previous group [6, 7], this was to be from using and Internal Combustion (IC) engine driving a generator. One of the aims this year was to determine whether or not such a concept would be feasible.

With the introduction of an internal combustion engine, the weight of the platform is increased. Therefore, the 5 electric fans used by the previous group would not achieve enough thrust to lift the platform. An attempt at using an IC engine for propulsion by the group in 2000 – 2001 concluded stating that such a method does not respond fast enough in order to correct instability. However, when run constantly, the thrust achieved is significantly greater than for the electric fans. Therefore a central ducted fan powered by a second IC engine is proposed for the platform. The intention is that this will generate enough thrust to justify its use and support the other engine with the perimeter electric fans as stability correction. An outcome whether such a method would be achievable was also intended to be reached by the end of the project.

Thanks to the generosity of BAE Systems, the project was loaned an Inertial Measurement Unit (IMU). Such a device incorporated three accelerometers, three electronic gyroscopes and 2 inclinometers to determine spatial position in the 6 degrees of freedom illustrated in appendix 2. The IMU was precision Engineered and as a result, the outputs were clean and incurred minimal drift. Through the construction of a decoder unit, the role of the IMU was hoped to improve the stability of the Platform.

With introduction of IC engines, the control of the platform was made more complex. The effect of fuel tanks in terms of fuel consumption and fuel motion resulted in a change in the way the weight is distributed on the platform. Additional effects from the engines also required a review of the current control system and improved where necessary.

The extra components such as the IC engines and IMU needed mounting on the structure requiring the existing one to be reassessed. The IC engines caused vibrations intense enough to sheer M4 bolts and so investigation of various mounting techniques was required. The balancing of the components was also important as this would affect the design and performance of the control system.

4. Project Organisation

The Flying Platform 2003 – 2004 project group comprised of 9 members. The project was governed by Dr. M.A. Jenkins and Dr. G.A. Lester who provided guidance where necessary. Table 4.1 lists all the group members with the areas in which they contributed to the project.

Name	Responsibilities
Liam Dushynsky (Project Chairman)	Project Management IMU Decoding Propulsion Testing Genset Testing
Richard Forder	IMU analysis IMU interfacing IMU testing
Richard Holbrook	Mechanical Test rig design Mechanical Test rig construction IC Engine research and selection Propulsion Testing Genset Testing
Rebecca Hughes	Initial Thrust Testing Control Theory Control System Design
Kevin Lowis (Project Treasurer)	Control Theory Control System Design Control System Construction
James Mackenzie – Burrows (Project Secretary)	Electrical Power Generation Electrical Test rig design Electrical Test rig construction Propulsion Testing Genset Testing
Jody Muelaner	Mechanical Theory Design of custom central fan
Christopher Poczka	Control Theory Propulsion duct analysis Propulsion duct design Propulsion Testing Structure
Alex Tombling	PIC Design and programming Initial Thrust Testing Electrical Test rig construction Propulsion Testing Genset Testing

Table 4.1: The 2003 – 2004 Flying Platform Group

5. Project Management

5.1 Introduction

In a project as diverse and as complex as this, effective management was of key importance. With 9 members in the group, meetings were required in order to express opinions and share ideas. These meetings also aimed to maintain a group structure and prevent fragmentation. At the first meeting, a Chair person was elected whose role was to co-ordinate the group to succeed in achieving the aims of the project. A comprehensive discussion on the overall project management can be found in the Chair report [9].

In order to maintain constant communication, it was decided that the group would hold two formal meetings every week throughout the first and second semesters. Monday morning meetings were used to discuss what had been achieved by group members over the weekend. Once progress had been determined, a course of action was then planned for the rest of the week. Thursday meetings were held with the supervisors, and invited guests, allowing the group to benefit from any advice given as well as providing the guests with feedback as to the progress of the project. Any specialist advice could then be researched over the weekend by individuals in preparation for the Monday meeting.

5.2 Role of the Secretary

The project secretary maintained minute keeping throughout all of the formal meetings. These can be found in 2 volumes [10, 11]. Initially minutes were endeavoured to be published by the same afternoon as the meeting. However, as the project progressed, the priority throughout the working day needed to be focused on the progression of practical work. As a result, minutes were available to all by the next working day. An established layout was agreed on by the third week, which was then adhered to for the duration of the project. A copy of the minutes from a randomly chosen meeting can be found in Appendix 3.

Informal meetings could be held in the workshop designated to the project. In order to make any important information available, it was decided that the group would benefit from using the University's WebCT system. The secretary managed this, allowed designated users to log in to shared files from any location, ensuring a constant availability of such information by all. Once established, WebCT was the distribution method for the minutes to all group members with the exception of supervisors and guests. To these, the minutes were delivered to either in person or via pigeon holes.

5.3 Role of the Treasurer

In order to maintain the finances of the project, a Treasurer was appointed through whom all purchases were made. Expensive purchases including the IC engine required the approval of the supervisors before approval was given.

Details of the financial management can be found in the treasurer's report [12].

5.4 Sectional Organisation

As the project began to progress, 4 distinct sections became apparent. All members were part of these groups but not restricted to just one. The Chair appointed sectional managers who would coordinate the teams and liaise together to ensure a continuous flow of information. This sectional structure is shown in table 5.1.

Section	**Group Members**
Control / IMU (Included control theory and testing)	Kevin Lowis (Section leader) Richard Forder Liam Dushynsky Rebecca Hughes
Propulsion (Included central fan IC engine testing, prototype duct testing and design for custom central fan)	Richard Holbrook (Section leader) Alex Tombling James Mackenzie – Burrows Christopher Poczka Jody Muelaner
Electrical Power Systems (Included Genset and power distribution)	Alex Tombling (Section leader) James Mackenzie – Burrows Richard Holbrook
Structure	Christopher Poczka (Section leader) Jody Muelaner

Table 5.1: Sectional Organisation

Throughout the majority of the project, this organisation was effective in terms of productivity. Information was transferred between sections well. However, towards the later part of the project, commitment from various members was not always strong and progress begun to deviate from the critical path of the project plan [9]. The chair responded to this by assigning more people to the critical path tasks which were not complete. Unfortunately by the end of the project, and at the time of writing, not all the tasks were completed.

6. Work Completed

All work in this report was completed during the course of the 2003 – 2004 academic year. As explained, each member focused on different aspects of the project depending on the section they were part of. After much deliberation and discussion throughout the year, it was decided that the resulting Platform should consist of the following (see Appendix 4 for a diagrammatic version):

- A new structure such that the centre of mass is made as low as possible to allow a more simple method of stability correction.
- This stability would be achieved through the four perimeter electric fans introduced by last year.
- Improve the overall thrust by developing a central fan driven directly from an IC engine mounted in the centre of the Platform.
- Introduce a second IC engine, directly driving a generator, to provide electric power to the perimeter fans and all the onboard electronics.
- Further improve the stability of the platform by consolidating the separate accelerometers and gyroscopes into the IMU and appropriate decoding circuitry.

The author of this report primarily completed the following work in the areas of electric power generation and distribution and this is discussed in this report. However, as already explained, for such a complex project, it was impractical for each member to work individually. A considerable amount of assistance was given to the propulsion section working on the central fan design in light of several problems which were encountered [13, 14].

6.1 Electrical Power Systems

As coordinator of achieving electrical power, the author was guided by the aim of the task; to produce maximum power from minimum weight. Different methods of power production were experimented with and will be discussed in this section. The initial starting point was to determine how much power was required by all electrical and electronic components of the platform. The perimeter fans would be providing a substantial level of thrust but also would be consuming the highest amount of power. It was evident from previous experiments [15] that as the speed of these fans increase, so did the level of current consumed. Therefore, if the level of thrust needed was determined, then the total power needed to be produced could be calculated. However, the thrust was dependant on the weight of the platform. This could not be calculated until all the components were decided upon and mounted on the structure. Very quickly, it was realised that each section of the platform became dependant on the outcome of another. In order to prevent the progress of the project reaching a grinding halt then assumptions needed to be made. After committing to an OS Max 91 engine for the central fan and basing the weight of the structure the existing one, an estimation of the total weight was made including payload. This was to be 8.3 kg inclusive of payload [16]. The central fan could theoretically provide 6 kg of thrust which meant that the rest had to come from the perimeter fans.

6.2 Thrust Testing of Perimeter Fans

Testing of one of these fans was already conducted by the previous group. However, as the outcome of testing was fundamental to the project, the test was repeated by this year's group. Details of the test rig used are discussed by R. Holbrook [13]. Several results were recorded and calculated during the course of the testing and these can be found in Appendix 5. Out of these, the most significant to the power production design can be seen in figure 6.1. The thrust was measured by placing a pair of scales under the opposite end of a pivoting arm to which a single fan was mounted. The power was calculated from the following equation:

$$P = I \cdot V \qquad \text{(eq. 1)}$$

Where: P = Power (Watts)
I = Current (Amps)
V = Potential Difference, P.D. (Volts)

The fan was powered by one 12 V, 100 Ah lead acid battery. Three of these batteries were used during tethered flight by the previous group. The variables I and V from equation 1 were measured from the positive and negative connections to the speed controller of the motor. Details on the speed controller are discussed later in this report. One point to note is that as the currents from the battery were significant, a series ammeter could not be used. This was resolved by using a clip on ammeter.

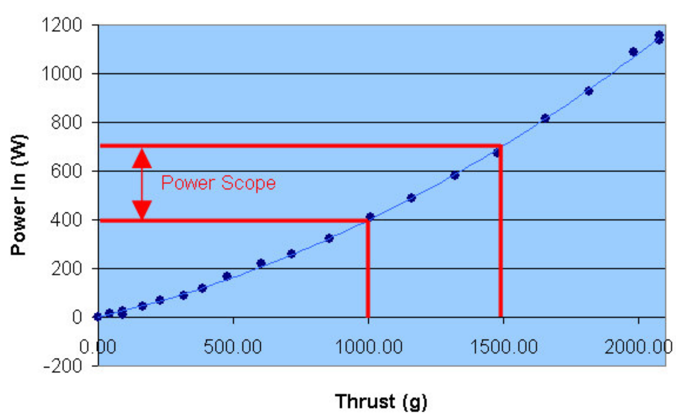

Figure 6.1: Electric Perimeter Fans, thrust vs. power consumed

As the sum total of the thrust produced from the fans must be 10 kg, this requires the perimeter fans to produce a minimum of 1 kg of thrust. However, during flight, the platform would not be able to meet the demands of any surge requirements. Such occurrences would be likely if the platform needs to recover from a disturbance or increase in height. In order to cope with this flexibility, a maximum thrust level was stated at 1.5 kg. Therefore the power supply designed must be able to provide between 1.6 kW and 2.8 kW for the fans with additional consideration for the onboard electronics. Several options were available in order to solve this problem. The two which were investigated are power storage and power generation. These are discussed in sections 6.3 and 6.4.

6.3 Power Storage Methods

6.3.1 Batteries

Significant advances in battery technology have allowed these to be considered for use as an energy supply in such an application. During the stability testing undertaken by the previous group, three 12V 100Ah Seal Lead Acid (SLA) batteries were used to provide the currents required by the perimeter fans. These fans are governed by a Schulze 32.55 speed controller into which the specified potential difference can be varied between 12V and 36V. Table 6.1 illustrates the four extreme scenarios based on these variable potential difference requirements and also the variable power requirements. A decision was agreed by the group that the battery unit needs to supply the required power for under 3 kg otherwise other options need to be explored.

Power Required by fans (W)	P.D. into speed controller (V)	Resulting Current (A)	Amp hour requirement of battery over a 20 minute flight (Ah)
1600 (min)	12 (min)	133	44.3
1600 (min)	36 (max)	44	14.6
2800 (max)	12 (min)	233	77.7
2800 (max)	36 (max)	78	26

Table 6.1: Battery ratings under different scenarios

From research, it was found that the batteries which offer the greatest variety are Nickel Cadmium (Ni-Cd), Nickel Metal Hydride (NiMH), Lithium ion (Li-ion) and Lead-Acid.

Ni-Cd batteries have been commercially available since 1947 [17] make them one of the oldest technologies which are still in use today. With a reputation for being one of the most “rugged” rechargeable batteries, they work well in different situations. However, they require pulse charging over a 2-4 hr period which means that persistent trickle charging by the platform is not an option. They also require maintenance of regular complete discharge in order to prolong their life. If this is not done then Cadmium crystals form which may pierce the separator between the anode and cathode resulting in deep discharge. This is known as the memory effect meaning that the battery will “remember” about previous discharges and will never fully recover to its original rated voltage. Although recommended with a C rating of 1 they are capable of meeting a peak C rating of 20. This means that a 1 Ah cell could deliver 1 A over a 1 hour period but can deliver 20 A over 3 minutes without damaging the battery. From a cost point of view, Ni-Cd batteries are the cheapest available and would be ideal for testing purposes. However, it has only been possible to source a 12 Ah Ni-Cd pack weighing in excess of 6 kg [18].

NiMH batteries were introduced in the early 1990s with the promise that they were the replacement to Ni-Cd. With no cadmium, they were more environmentally friendly and boasted a higher energy density of 60 Wh/kg. Again, these batteries do not appreciate trickle charging and must be well maintained in order to preserve longevity. After a visit to BAE systems, investigation of the power technique behind the Segway [19] human transportation vehicle revealed that they use two 60 NiMH cell packs with an integrated control unit to monitor their health and state. These packs run at a nominal 72 V and are rated at 40 Ah [20]. These would meet the requirements of the flying platform but no information could be obtained from Segway as to their weight. After contacting SAFT, who were responsible for developing the Segway batteries, they concluded that a 21 NiMH battery with a terminal voltage of 25 V and a capacity of 27 Ah would be the only solution [21]. However, this would weigh in the region of 9 kg making it impractical for use on the platform.

Li-ion batteries are relatively new with Sony commercialising the first rechargeable cell in 1991 [17]. A the time of writing, energy densities are more than twice that of Ni-Cd at 150 Wh/kg , making them an attractive alternative for use in portable equipment such as laptops and mobile phones. However, they are fragile. Protective circuits are needed to prevent damage from overcharging, excessive demands on current and high discharge rates. With the high demand for current from the platform then these cells would not be suitable in responding to an input disturbance. Even though the power to weight ratio is preferable compared to Ni-Cd it is still not enough to meet the strict requirements of the platform. With further development of the chemistry then these batteries may provide a solution to this issue in the future.

Lead Acid batteries come in two types: “sealed” and “wet”. Wet batteries are found in cars and require maintenance by topping up the charge with deionised water. SLA batteries are maintenance free. Four types of Lead Acid battery exist which were researched for feasibility. They are listed as follows:

- Cyclic lead acid batteries can be heavily charged and discharged but provide a low level of power.
- Standby lead acid batteries can be trickle charged until they are needed. They are then able to deliver high currents with stable voltages. Large scale batteries are used in industrial power systems to prevent fluctuations in the event of the power supply switching.
- Motive batteries are used in applications where power is required for a specific purpose such a vehicle where the current drawn will be more or less the same.
- Automotive batteries are the wet lead acids found in cars. These provide the large currents to start the engine and then supply any electronics whilst constantly being trickle charged by the dynamo.

From the characteristics listed above a SLA battery would be the most suitable. However, their weight is the limiting factor and energy densities are typically 45 Wh/kg. Correspondence with various suppliers revealed clearly that SLA batteries are too heavy for such an application. This is shown in table 6.2 overleaf:

Supplier	Battery Model	Rated Voltage (V)	Capacity (Ah)	Weight (kg)
CPC Battery Service	MPC 17/12	12V	17	6
CPC Battery Service	-	24	38	15
Battery Specialists	-	12	30	10
Batteries Direct	EW230	24	230	70
Batteries Direct	EW75	24	75	20

Table 6.2: Comparison of available lead acid batteries from direct correspondence

Therefore in conclusion to this study, batteries are currently not a suitable option for powering this particular flying platform. However, the continued development of Li-ion batteries may result in energy densities which are suitable for such an application.

6.3.2 Ultra Capacitors

Typical capacitors only hold small amounts of change and are rated in the picoFarad (pF), nanoFarad (nF) and microFarad (μF) regions. Ultra capacitors are based in the Farad region making them the ideal solution for delivering high levels of power in a situation where a battery is not required. Table 6.3 directly compares the characteristics of a lead-acid battery with an ultra capacitor.

	Lead Acid	Ultra Capacitor
Charge Time	1 – 5 hours	0.3 – 30 seconds
Discharge Time	0.3 – 3 hours	0.3 – 30 seconds
Energy (Wh/kg)	10 – 100	1 – 10
Cycle Life	1000	>500,000
Efficiency	70% - 85%	85% - 90%

Table 6.3: Comparison of Ultra Capacitors with Lead Acid Batteries

Ultra capacitors decay linearly unlike lead acid and other electro-chemical batteries. This means that the capacitor is only useful over a short period of time figure 6.2 illustrates decay trend for the different energy sources:

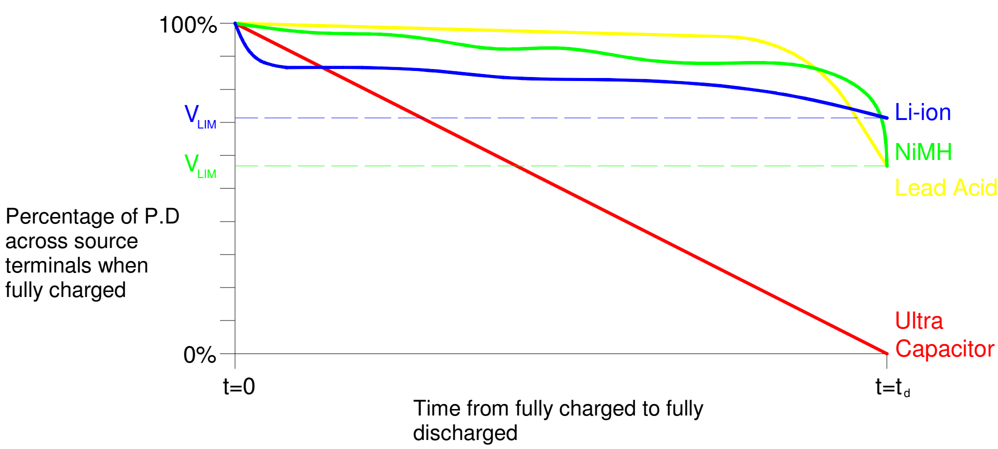

Figure 6.2: Decay trends for different energy storage sources

For the types of energy storage sources discussed, figure 6.2 shows the decay trend that the source follows from a fully charged state to a fully discharged state as recommended by the manufacturer. Unlike ultra capacitors, electrochemical sources must not be deep discharged to avoid damage to the cell structure. Therefore, V_{LIM} will be defined by the manufacturer to be the lowest level at which the source can be operated at. However, it can be seen that these sources remain above 70% of their fully charged voltage for over 90% of their discharging time. Ultra capacitors decay so rapidly the load they are supplying may have switched off before they are even 40% discharged.

With such short discharge times, ultra capacitors are not suitable as battery substitutes. Applications such as hybrid engines and uninterruptible power supplies (UPS) have seen ultra capacitors used in parallel with a battery in order to meet any surge current requirements which the power supply could not meet on its own. However, the main disadvantage of using an ultra capacitor for the flying platform is weight. The Tavrima ESCAP 10/42 can provide 62 A at 42 V but at a cost of 10.5 kg. Unlike batteries, smaller ultra capacitors cannot be connected together in series to increase the total potential difference thus limiting the choice available. Additional voltage balancing circuitry is required in this case. A summary given to the group the findings from the research of ultra capacitors can be seen in Appendix 6.

6.4 Power Generation

It has now been proved that a platform power supply using energy storage methods is not possible with the current technologies available. If it were possible to use ultra capacitors or lead acid batteries then a dynamo or generator would be needed anyway to maintain charge levels. In light of the impressive capabilities of the OS Max 91 ducted fan IC engine [13], it was decided to investigate the possibility of using one of these to drive a generator to produce all the power without the need to store it. Such a commitment required close cooperation between mechanical and electronic disciplines and from this the Electrical Power Systems sub group was formed. Research was undertaken for the suitability of using dynamos or alternators [25] but concluded that these were too heavy. As a result, it was decided to investigate the possibility of using an electric motor driven in reverse to produce power.

6.5 Motor theory

A current carrying wire will deflect a compass needle. This was first noticed and studies by Oersted in 1819. From this it was proved that a current flowing in a conductor creates an electrostatic field perpendicular to the conductor as shown in figure 6.3. The direction of flux around this conductor is represented by the well known “screw rule” and originates from atomic spin. (Note: During the course of this theory, conventional current flow will be used and not electron flow theory.) When such a conductor is placed in a magnetic field, it will experience a force. This will be proportional to the velocity of the charges in the wire, proportional to the strength of the magnetic field and in a direction perpendicular to velocity and field [26]. The magnitude of this force is given by equation 2.

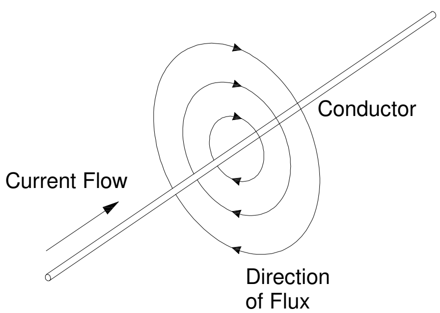

Figure 6.3: Flux lines around a current carrying conductor

$$|\underline{F}| = q \cdot |\underline{v}| \cdot |\underline{B}| \cdot \sin\theta \qquad \text{(eq. 2)}$$

Where:
- $|\underline{F}|$ = Magnitude of the resultant force (in vector form)
- q = charge on an electron
- $|\underline{v}|$ = velocity of electron (in vector form)
- $|\underline{B}|$ = Magnetic Flux Density (in vector form)
- θ = angle between the velocity vector and the flux density vector

The direction of the magnetic field is best demonstrated in diagrammatic form. In figure 6.4 it can be seen that the sum total of flux is greater above the conductor than below it. The magnetic flux lines do indeed “bend” around the conductor and therefore will exert a force in the direction indicated. The three variables are current, magnetic field and direction of force. All three are separated by 90° and if the direction of two is known then the third can be determined by Fleming's Left Hand Rule.

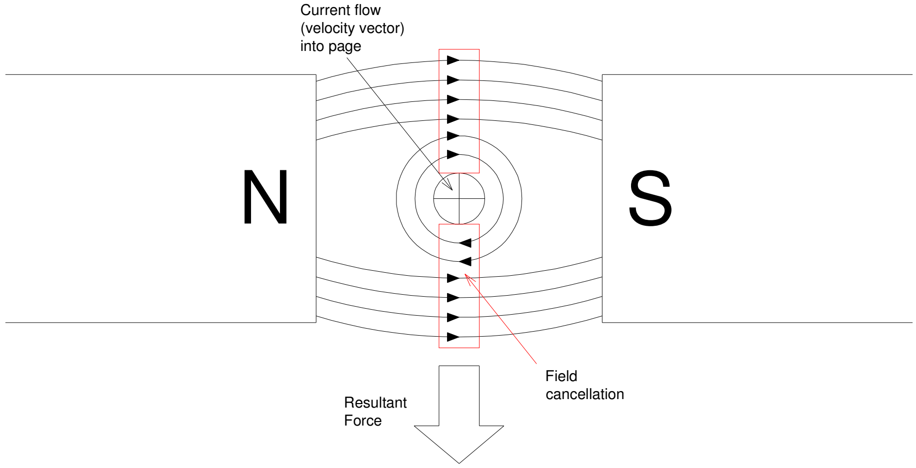

Figure 6.4: Effect of a current carrying conductor in a magnetic field.

A conductor is effectively a "tunnel" for charge to travel. The charge flowing in the conductor is given by equation 3

$$q = I \cdot t \qquad \text{(eq. 3)}$$

Where: q = Charge in a conductor (C)
I = Current in conductor (A)
t = Time for the current to flow (s)

Re-writing equation 2 with this definition of charge gives:

$$|\underline{F}| = I \cdot t \cdot |\underline{v}| \cdot |\underline{B}| \cdot \sin\theta \qquad \text{(eq. 4)}$$

or

$$|\underline{F}| = I \cdot L \cdot |\underline{B}| \cdot \sin\theta \qquad \text{(eq. 5)}$$

where: L = the length of the conductor

Ideally, in a motor, the "sin θ" term should be 1 so as to not to reduce the resultant force, $|\underline{F}|$. The closer that motors can be manufactured with conductors perpendicular to the magnetic field, the more efficient they are. In this condition, they obey equation 6, also known as the Motor Equation

$$|\underline{F}| = B \cdot I \cdot L \qquad \text{(eq. 6)}$$

6.5.1 DC Motor

In a basic DC motor, continuous rotation is achieved through the use of split ring commutators. In effect, these turn the DC input into a square AC signal. However, the output torque from a DC motor does not remain continuous. Figures 6.5 to 6.7 illustrate the reason for this variation.

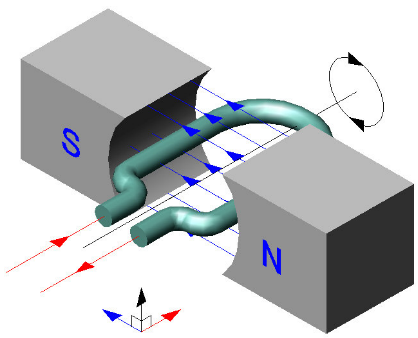

Figure 6.5: DC motor, stage 1

A motor is constantly trying to force a current carrying conductor in the direction indicated by Fleming's left hand rule. When the motor is in the orientation shown in figure 6.5, the tangential direction of motion is parallel to this force. As a result, this is where the greatest amount of torque occurs. It follows that:

$$F = BIL$$

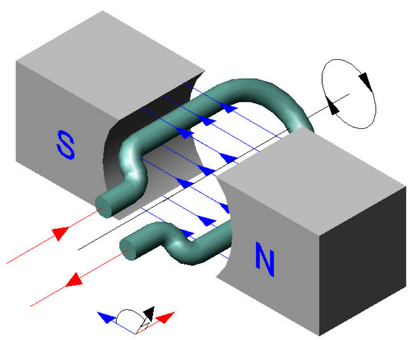

Figure 6.6: DC motor, stage 2

As the motor rotates, the electromagnetic force on the winding is no longer acting parallel to its direction of motion. Only a component of this force is acting. At 45°, the magnitude of this force is given by:

$$F = BIL \cdot \sin 45^\circ$$

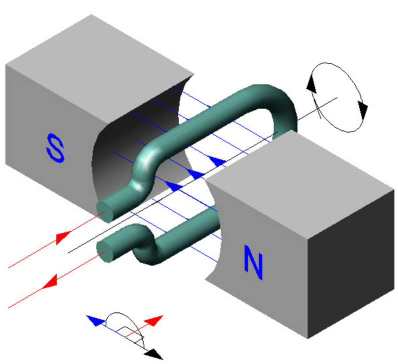

Figure 6.7: DC motor, stage 3

Finally when the direction of motion is parallel to the magnetic field, the windings on the motor experience no electromagnetic force. This is due to the following:

$$F = BIL \cdot \sin 180^\circ = 0$$

However, the motor continues to rotate due to its own momentum. This is also the stage where the commutators must reverse the flow of current so that the electromagnetic force is in the opposite direction. As a result, the torque obtained from a DC motor is sinusoidal as shown in figure 6.8.

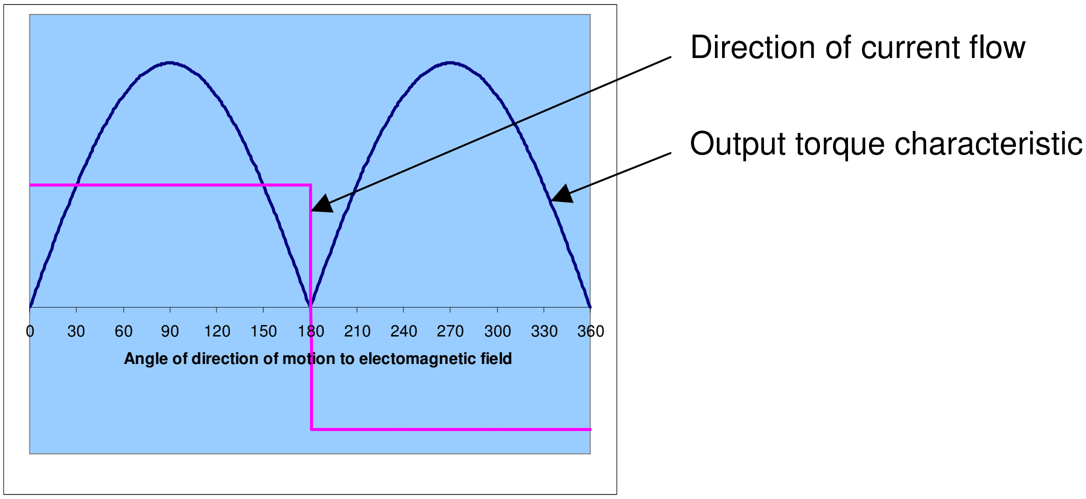

Figure 6.8: Current and torque characteristics of a DC motor

If it was not for the mechanical inertia of the motor, then this variation in the torque may lead to a jerky operation. DC motors were used by the 2001 – 2002 project group. These were Graupner Speed 600 BB Turbo 12V motors (referred to hereafter as the Graupner Motors) and were available to the group for experimentation.

Figure 6.9: A Graupner DC motor

6.5.2 AC Motors

As the current in an AC motor is continually reversing, there is no need for split ring commutation. Each end of the motor winding is directly connected to the source by means of slip rings. The speed of such a motor is varied by alternating the frequency of the AC signal at predefined amplitude. However, in the same way as for a DC motor, the torque of a single phase AC motor drops to zero twice during every cycle.

6.5.3 Three phase AC motors

The Plettenberg HP 220 motors were used by the previous year's group to power the electric fans as they could achieve in excess of 500 W of power at 16 V. This reason for this is due to the supply of 3 AC singles each of which is 120° out of phase. Due to the fact that each phase is zero when the others are not results in continuous torque supplied by the motor. 3 phase theory is discussed in depth in the following section. From a simplistic point of view, a 3 phase motor will always provide more torque than a single phase or DC motor. However, in order to achieve this, 3 phase motors require a significant quantity of power.

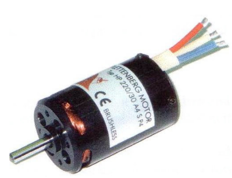

Figure 6.10: A Plettenberg HP 220 3 phase motor

6.6 Electrical Power Generation

It has been demonstrated that when a current is applied to a conductor in a magnetic field, motion occurs in the direction stated by Fleming's left hand motor rule. However, a back e.m.f. is generated in the opposite direction to this current flow as explained by Lenz's law. Therefore, if a conductor is passed through a magnetic field, it is found that a current flows from one end of the conductor to the other as a result of this induced e.m.f. As this exists in the opposite direction as for motors then Fleming's right hand rule applies in this case.

The magnitude of the e.m.f. induced is dependant upon; the flux density of the magnetic field (B); the length of the conductor passing through the magnetic field (l); and the velocity which the conductor cuts the magnetic field (v). Equation 7 illustrates the relationship between these variables.

$$E = B \cdot l \cdot v \qquad \text{(eq. 7)}$$

Therefore, it follows that if a motor with a high magnetic flux density is rotated at speed, a voltage will exist on the output terminals. If a motor is supplied with a certain level of electrical power (P1) then a subsequent mechanical power (P2) will exist when the motor rotates. The amount by which P2 is less than P1 depends on the efficiency of the motor. Supposing the situation is reversed and a mechanical power of P1 is put on the motor shaft. According to generator rule then an electrical power of P2 will be supplied to the terminals. Such a method was believed to be the solution to achieving a light weight power supply on the Flying Platform providing the motors exhibit high efficiencies. The only way to tell if this would work was to test.

6.6.1 Testing of Plettenburg HP 220 Motors

These motors were used by the previous group to power the propulsion fans. As the group were already in possession of the motors then the cost of the experiment was minimal. Details of the mechanical construction are contained with in R. Holbrook's report [13]. As illustrated in figure 6.11, two Plettenberg HP 220 Motors were mounted such that one was driving the other by means of a coupling on the motor shafts.

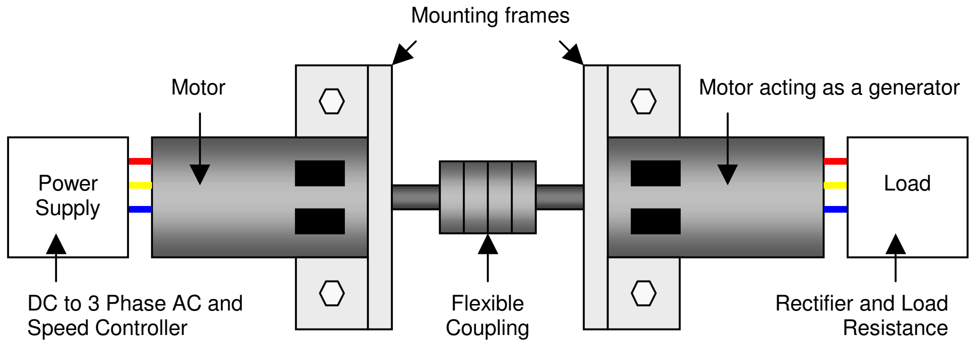

Figure 6.11: Rig for HP 220 Motor Testing

The Schulze 32.55 controller was used in conjunction with a PWM controller [25] to vary the speed of the motor. As the speed controller converts DC into 3 phase AC, the electrical power into the motor was calculated from the DC supply in the same way as for the thrust testing experiment in section 6.2. At this stage it was assumed that any loses in the speed controller would be negligible and that the full electrical power from the DC source was reaching the motors.

On the output terminals of the generator motor, a 3 phase signal was produced; this needed to be converted into DC in order to calculate the power output. Therefore, the rectifier circuit discussed later in section 6.8 was used. As earlier stated, electrical power is calculated by using equation 1. This implies that a current must be allowed to flow and so the rectified DC signal from the generator was connected to a load resistance typical to that of the Flying Platform. This was modelled by using a high current variable resistor.

The experiment was run at varying motor speeds and various load resistances. Care was taken not run the motor at excessive speeds. For this a mark was drawn on the coupling which was detected by a strobe in order to calculate speed. The results from testing this motor can be found in Appendix 7.

Conclusion to Plettenberg HP 220 Motor Testing

As can be seen from the results, at a load resistance of 1 ohm, typical to that assumed of the platform, the power obtained was over 370 W with an efficiency exceeding 96%. However, this efficiency was only displayed at high speeds. Therefore, if such a motor were to act as a generator then the mechanical source must be able to support this. However, at this stage, initial results were promising.

6.6.2 Testing of Graupner 12V Motors

These motors were available after use by the 2001 – 2002 group. Therefore another generator test was conducted at minimal expense. The Plettenberg HP 220 motors proved to be efficient in operation, therefore one was used to drive a Graupner motor as a generator as shown in figure 6.12.

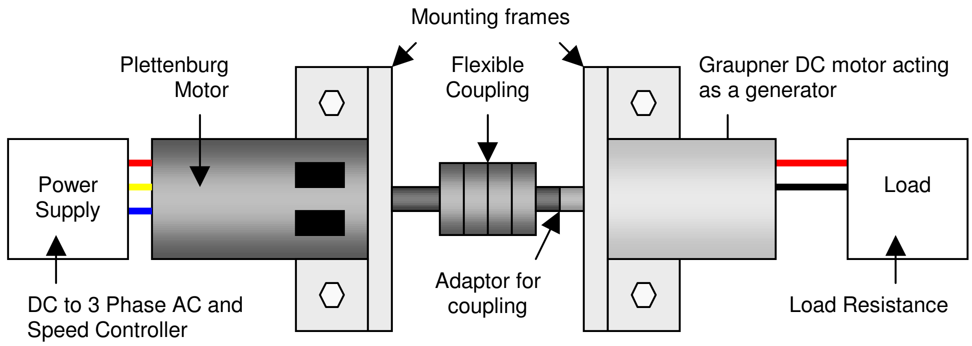

Figure 6.12: Rig for Graupner Motor testing

As the properties of the Graupner motor were more limited than the Plettenberg, care had to be taken during testing not to run it above its capabilities. In operation as a motor, the Graupner reached a speed of 20000 rpm at its maximum voltage of 12 V. Therefore, care was taken not to exceed this speed when run in reverse.

As a DC generator, the Graupner required no additional rectifier circuitry and could be directly connected to the load resistance.

The test was conducted in the same manner as for the HP 220 motors but with the speed limit of 20,000 rpm. The results from this test are shown in Appendix 8. The integrity of some of the results may be questionable owing to the quality of the adaptor between the generator and the flexible coupling. The motor shaft on the Graupner motor was of a smaller diameter but rather than purchase a new coupling for just one test, an adaptor was placed between the motor shaft and the coupling. This was satisfactory for the majority of testing with the exception of some low resistance loads. In these cases, the torque in the motor shafts and coupling would have been greater, causing the adaptor to slip occasionally.

Conclusion to Graupner Motor Testing

As can be seen from the results, the efficiency of this DC motor was low with a maximum power output of only 40.5 W. Therefore, it was concluded from this that a DC motor was not satisfactory for the requirements of the Flying Platform. For reasons explained in section 6.5.3, 3 phase motors are significantly more powerful than single phase or DC motors. Following the positive outcome of the Plettenberg tests, it was decided to research other motors which Plettenberg offer capable of providing greater power. From this, the HP 370/30/A2 S SL was chosen. This boasted a mechanical output power of 1467.6 W at a speed of 16135.8 rpm whilst delivering a torque of 86.9 Nm.

6.6.3 Testing of Plettenberg HP 370/30/A2 S SL Motor

Owing to the high expense of one of these motors [12], only one was purchase with the satisfaction that it would be adequate for the Platform's needs. Once arrived, this motor was tested in a similar fashion to the previous motors but using the HP 220 as the source. The test rig for this experiment can be seen in figure 6.13.

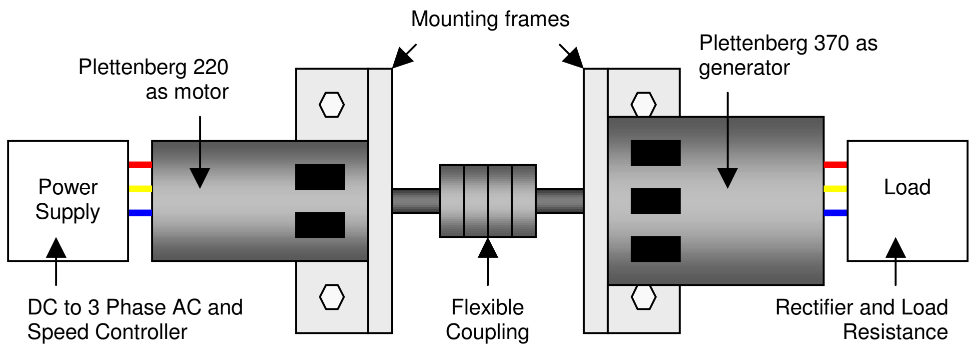

Figure 6.13: Rig Plettenberg HP 370 Motor testing

The test was conducted in the same fashion as for the HP 220 motors. However, excessive heat emissions from both motors were noticed at high speeds. The results from this test are shown in Appendix 9.

Conclusion to Plettenberg HP 370/30/A2 S SL Motor Testing

As can be seen from the results, efficiencies were low from this motor. However, it was agreed by all present during testing that this was due to the configuration of the test. The smaller HP 220 could not meet the power requirements of the larger HP 370/30/A2 S SL (hereafter referred to as the HP 370). With efficiencies specified in excess of 80% by the manufacturer, this motor had the ability to perform better. Therefore, the original intension of using an IC engine to power the HP 370 as a generator was developed. This unit was named the “genset”.

6.7 Three Phase Power Generation

6.7.1 Theory

In section 6.5.1 it was explained that when continuous DC is supplied to a basic motor, sinusoidal output torque was achieved. Here the opposite is true: a continuous mechanical input produces a sinusoidal electrical output. Figure 6.14 illustrates the behaviour of such a generator.

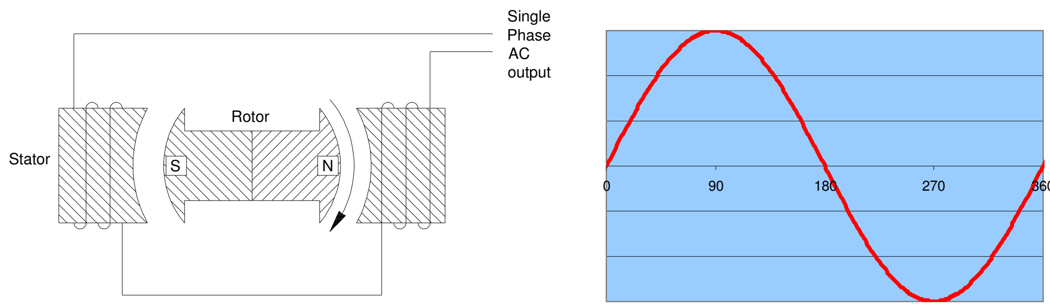

Figure 6.14: Output from a basic single phase generator

If the output voltage of a generator behaves in this sinusoidal fashion then the current drawn from the generator will as well. As a result, the power from such a generator will be zero twice during each cycle. Much can be gained if the Platform power supply is balanced out more. Indeed the manufacturers of the Schulze 32.55 speed controllers recommend that they should be supplied from a DC source [37]. Therefore, the power source needs to be able to reflect this. A single phase power source is not able to do this.

A three phase (3Φ) generator consists of a stator with all three separate windings symmetrically distributed around its periphery and an electromagnetic or permanent magnet rotor driven at synchronous speed by a turbine or engine. As it rotates, the rotor induces a sinusoidal voltage in the same way as above. With three individual windings, three sinusoidal voltages are induced. However, due to the orientation of these windings, each sinusoid is out of phase by 120°. This is shown in figure 6.15.

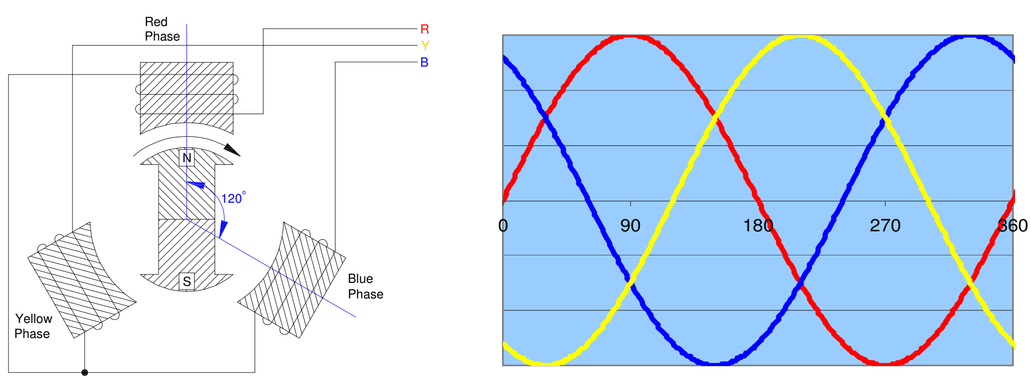

Figure 6.15: A 3Φ Generator and output sinusoids

It is important that each phase generated is loaded equally so that a balanced 3Φ system prevails. If this is true then the power from each sinusoid can be calculated from the following equations [28]:

$$P_{RED} = V_{RED}^2 / R \quad \text{(eq. 8)}$$

$$P_{YELLOW} = V_{YELLOW}^2 / R \quad \text{(eq. 9)}$$

$$P_{BLUE} = V_{BLUE}^2 / R \quad \text{(eq. 10)}$$

Plotted against time, the power for each phase can also be seen to be sinusoidal. The sum of all these sinusoids gives the total power of the 3Φ system which reveals that the total instantaneous power at all times is constant and equal. This is represented in equation 11.

$$P_{TOTAL} = P_{RED} + P_{YELLOW} + P_{BLUE} = 1.5 \cdot \frac{V^2}{R} \quad \text{(eq. 11)}$$

6.7.2 Winding of three phase sources and loads

3Φ motors and generators may be wound in one of two ways: Star or Delta. The difference between these windings is discussed here. Although the individual outputs from each phase are the same regardless of the internal wiring, it is important to note that each type behaves very differently when all phases are working together.

Star Windings

In a star configuration, the three windings share a common node called the “neutral node” as shown in figure 6.16. If the system is correctly balanced, then the total of all the currents flowing from this central node will be zero. In large scale applications, this neutral node is connected to the equivalent node on the 3Φ equipment it is supplying. This connection does not necessarily have to be made and is only used if the system potentially becomes unbalanced. A star wired 3Φ supply driving a star wired 3Φ motor, for example, will not need to make this connection as the system is perfectly balanced.

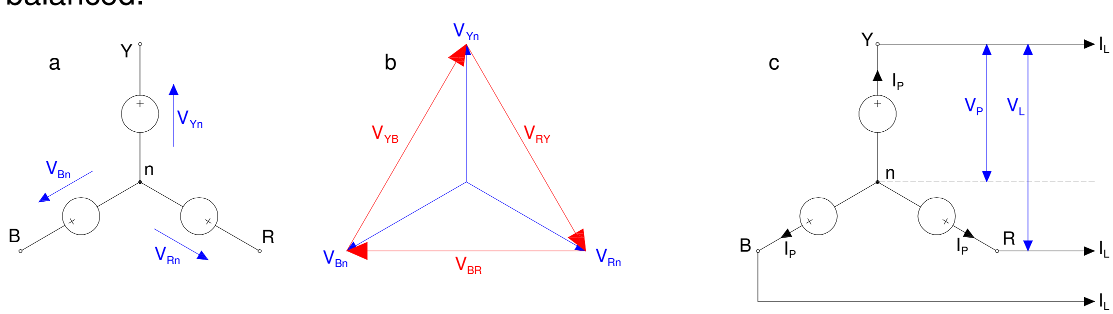

Figure 6.16: Star Phasors and wiring

As the current from the node point is zero, then at any one time, the sum total of currents in all phases will be zero. For each phase, the current flowing from the star point will be the same as for the source, seen in figure 6.16c. Therefore the following is true of star wired 3 phase systems:

$$I_P = I_L \qquad \text{(eq. 12)}$$

As the potential of the node is not "seen" by the load then potential difference can only be between phases. As these are 120° out of phase then phasor geometry can be used to find the solution. This is shown in figures 6.16b and 6.16c. It follows that the relationship between the source PD, V_p and the Load PD, V_l is given by:

$$V_L = \sqrt{3} \cdot V_P \qquad \text{(eq. 13)}$$

Therefore, using star wiring, a greater line PD can be achieved than from the individual sources. However, the current is the same. This makes star wires suitable in applications such as electrical power distribution where larger currents would require larger, heavier, more expensive conductors to transmit the same amount of power. Keeping the current the same but increasing the PD improves efficiency by typically 150% [29]. Also, the negative node can be supplied to consumers providing them with a 240 V or a 415 V (√3.240) supply depending on their requirements. This also has the added advantage that the 3 phases do not have to be strictly balanced by the consumer.

Delta Windings

In a delta configuration, there is no central node point. The three sources are connected together so that the negative side of one is joined to the positive of another. As a result, the configuration shown in figure 6.17a is achieved.

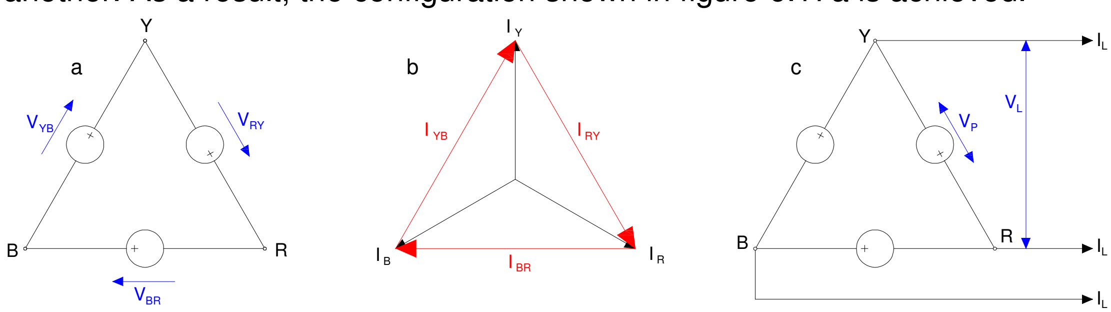

Figure 6.17: Delta Phasors and wiring

Due to the configuration of delta wiring, the potential difference across each phase is the same as each source, as shown in figure 16.7c. Therefore, for three phase delta generators:

$$V_I = V_P \qquad \text{(eq. 14)}$$

The sum total of all the currents in all three phases at any one time is zero as before with the star wiring method. When examining each phase in turn, it can be seen that each delta point does not directly come from one source. In the same way that the voltages in a star system were 120° out of phase, the current is now out of phase. Therefore, phasor geometry can be used to calculate the current in the output lines. The relationship is shown in equation 15.

$$I_L = \sqrt{3} \cdot I_P \tag{eq. 15}$$

Therefore, using a delta winding, greater total currents can be drawn compared to what each source can supply. The PD between the phases remains the same. This makes delta configurations useful for motors where greater currents will be needed from the lines as the torque increases. However, the current through each of the phase winding will be less. This allows motors to be constructed with thinner wire windings and reduces the heat generated.

Power Output from Star and Delta Windings [28]

The Power from each phase of a 3Φ generator is the product of its PD and Current flow. In the case of a star system this will be:

$$P = V_P\sqrt{3} \times I_P = V_P I_P \sqrt{3}$$

In a delta system the power produced is the same:

$$P = V_P \times I_P\sqrt{3} = V_P I_P \sqrt{3}$$

This proves that the same power can be achieved from either a star or a delta wired generator. The choice of wiring used depends on the application. Typically star wiring is ideal for generation as the resulting currents are low. Delta wiring of motors then allows a more efficient and cooler operation.

6.7.3 Conclusion of 3 Phase power research and its role on the Flying Platform

From this, it was possible to determine that the Plettenberg HP 370 motor was wired using a delta configuration which is ideal for use as a motor. However, in the role of a generator, achieving high voltages will be difficult. Providing that a level similar to that required by the HP220s can be achieved, there should theoretically be ample current available.

6.8 AC to DC conversion

Due to the nature of the Schulze 32.55 speed controllers, the 3 phase supply cannot be directly fed from the generator to the motors. The output of the generator needed to be converted to a stable DC for use as the input to the speed controllers and all the onboard electronics. The simplest form of AC to DC conversion is achieved by using a half or full bridge rectifier. In a 3 phase system, the full bridge rectifier can be extended as shown by the circuit in figure 6.18.

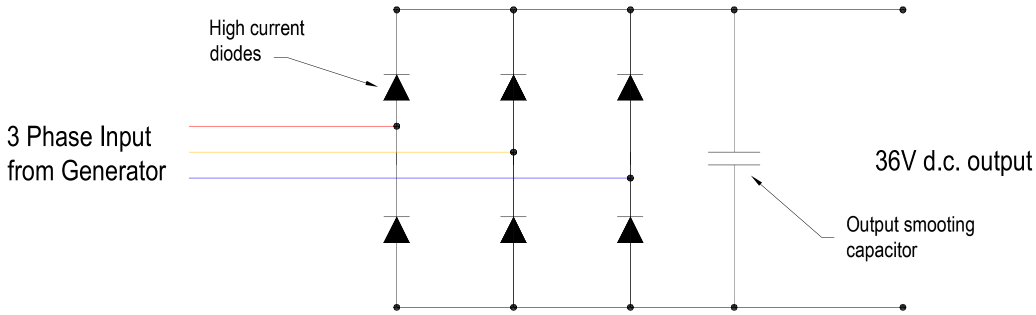

Figure 6.18: 3 phase AC to DC rectifier circuit

Two rectifier circuits were built. The first was built on strip board and could handle currents up to 60A. This was used for initial testing purposes. Following this, a 120A version was built for the final application as the perimeter fans would draw more than 60A of current when responding to stability disturbance. This circuit had to adopt a different construction than the first. As the generator was wired in delta form, comparatively high current levels would be drawn for a lower voltage. This would generate heat and so sinks were mounted on the diodes. The tracks on strip board would also not be able to handle such demands and so the final unit with 6.0mm^2 stranded cable shown in figure 6.19 was built. Once tested, this unit could be scaled down in weight and size for final application on the platform.

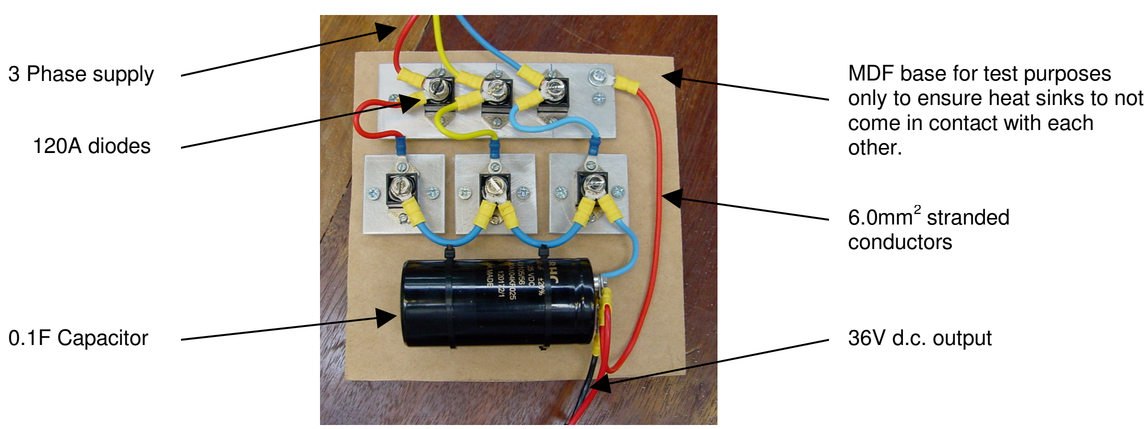

Figure 6.19: Final high current rectifier for testing purposes only

6.9 Genset Development

Following the understanding of electrical power generation and rectification, the genset could be built can tested. Such a design required close association between electronic and mechanical disciplines in order to develop a unit which would function correctly. The genset was to run in a configuration shown in figure 6.20.

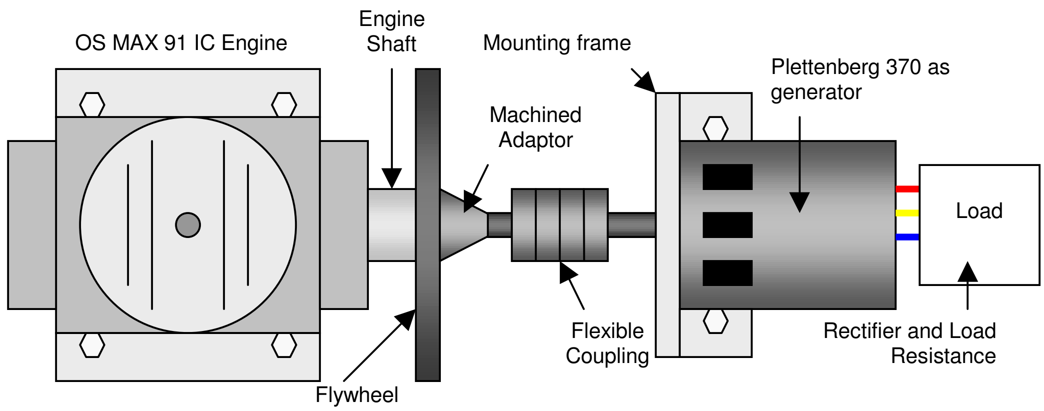

Figure 6.20: Genset Configuration

One of the initial problems which required a solution was how to start the engine when in this configuration. As discussed in detail by R. Holbrook [13], OS Max engines are either pull started or have an extra starter module attached to the shaft. This idea of using this additional module was discarded due its addition of extra weight. The issue of starting this IC engine is discussed in the following section.

6.9.1 IC starters

Consideration was made in how to restart the engines during flight in the event of failure. However, in order to achieve this, a lead acid battery would have to be mounted on the platform resulting in the weight of the platform being greater than the thrust available to lift. The control group also argued that an in flight starter would be pointless as the platform will never be able to restart in time to prevent itself crash landing. However, there is a safety concern here as well. Starting the IC engines manually requires close contact with the platform. In order to minimise personal risk, an idea of starting the platform from an umbilical was conceived. Due to the nature of the configuration of the genset, the Plettenberg HP 370 will have to momentarily act as a motor to turn the engine. This was to be fed by a three phase supply from the umbilical. Once this engine has started, the Plettenberg HP 370 will then serve as a generator supplying electrical power to the on board electronics and perimeter fans. Once online, the platform will detect that the central ducted fan IC is not running from a control circuit and activate a motor to start it. A block diagram of this concept as proposal to the group is shown in Appendix 10.

As the concept of using an IC engine to generate power was in its first stage of development, it was decided that the starter idea for the central fan IC engine should not be pursued this year. However, the genset IC engine needed to be started by this method in order to allow testing to begin.

6.9.2 Three Phase Umbilical Starter System

A 3Φ Mains Supply Starter

As explained in section 6.7.2, many consumers are supplied with a 3Φ electrical system operating at 50Hz. This supply could be used in a simple and effective way to start the genset IC engine. By using an array of transformers, the amplitude of the mains supply can be reduced to the 36V required by the motor. Figure 6.21 shows the method to connect 3 transformers to reduce the voltage of a 3Φ supply. In effect, the windings of the three transformers are connected in a star formation. In effect, this unit is the same as a generator but rather than mechanical power as the input, electrical power is used instead. Star windings are used to increase the voltage but not the current. In this way, the transformers remain cooler and can be smaller in size.

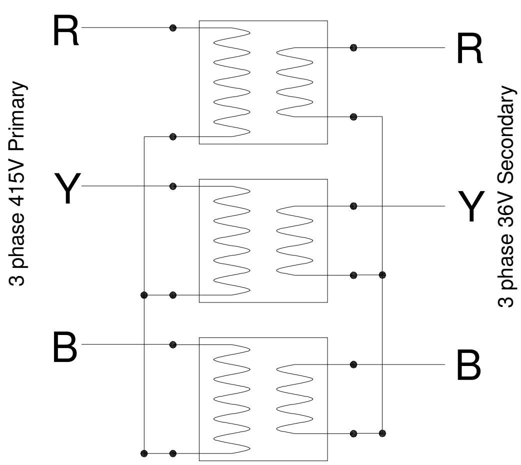

Figure 6.21: A Three Phase transformer

When the motor starts the engine, it will immediately reverse roles and become a generator. To avoid damage to the circuitry and the motor, this moment at which the engine starts needed to be detected and used to disconnect the power supply from the umbilical. For this, a Residual Current Device (RCD) was considered as a possible solution. In normal operation, the total current flowing at any one time will be zero providing that the load is balanced. When the engine starts, the genset will try to force anther 3Φ signal down the umbilical against the existing supply. Therefore, the phases through the RCD will become irregular and disordered. This will be seen as an imbalance by the RCD and it is hoped that it will cut out thus disconnecting the ground supply.

The concept of using an RCD and mains 3Φ supply was not used as it was felt that there was a safety concern dealing with lethal 415 V supplies. From a logistical point of view, this would also mean that the platform could only be started inside a building or at least somewhere where there was a 3Φ mains outlet. Such a method would be impractical for use in reality.

A Transistor Starter

It has been seen that mains 3Φ supplies are not portable or often available at locations where such a Flying Platform may wish to be started. Resorting to using a generator is impractical since this will take more time, effort and expense to move than the platform itself. DC SLA batteries are easily transportable and can achieve currents needed for such a starter circuit. From research and discussions, it may be possible to design a 3Φ starter circuit which is powered from such a DC battery. In effect, this would be a simplified version of a Schulze 32.55 speed controller.

A rudimentary 3Φ signal can be developed using a Peripheral Interface Controller (PIC) as discussed by A. Tombling [25]. However, the outputs from the PIC are rated at 25 mA max at 5 V. A method of using this small level of power to control the high currents required by the motor was devised by using power transistors. However, there are currently no power transistors available which can manage such high collector current from such a small base current. Therefore, MJ11015 npn Darlington pair transistors were used. According to the manufacturer's specifications and various calculations, it was possible to handle a 20 A collector current from a 4.4 mA base current. This required the use of a 24 V DC battery.

The resulting output from the PIC was such that current was drawn into the motor through one phase and released through the other two. This sequence was continued through each phase allowing rotation of the motor. The resulting connections to each motor phase for 1 cycle are shown in table 6.4.

Red Phase	Yellow Phase	Blue Phase
+24V	0V	0V
0V	+24V	0V
0V	0V	+24V

Table 6.4: 3Φ Generated from PIC

For each phase, an arrangement shown in figure 6.2.2 was used to control the flow of current either into or out of the motor. Both conditions are demonstrated. From this it can also be seen that care had to be taken not to ensure that both Darlington transistors were activated simultaneously. If this occurred, there would be a direct short circuit across the terminals of the battery. The full circuit diagram is shown in Appendix 11.

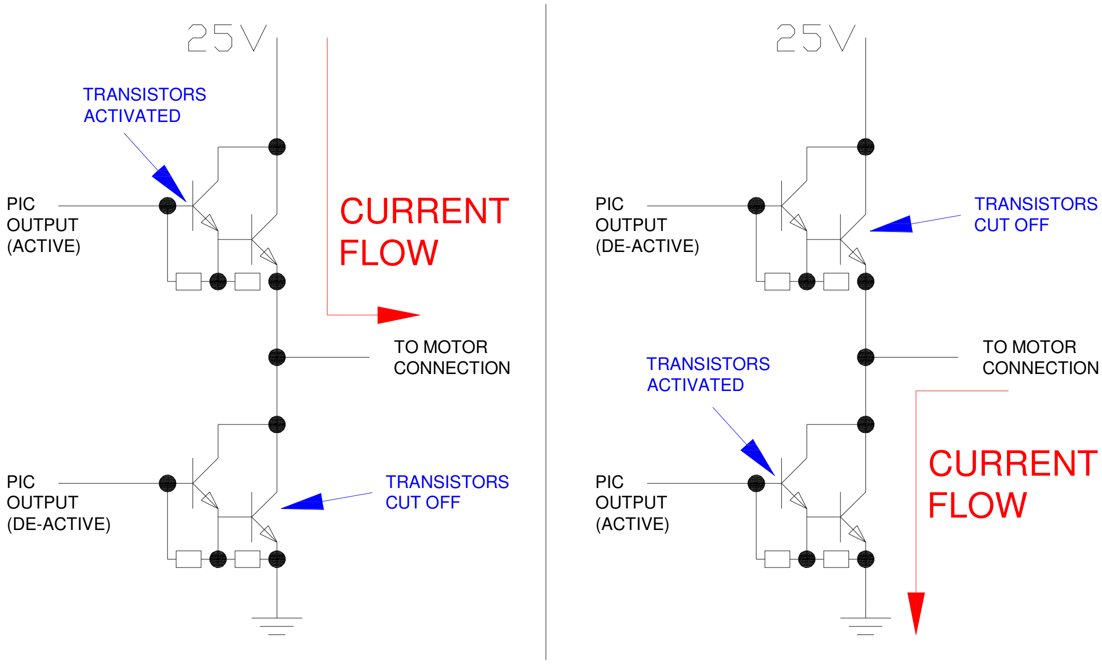

Figure 6.22: The two conditions of current flow either into or out of the motor

Testing of Transistor starter circuit

The initial test was unsuccessful owing to the different roles which the Darlington transistors play for each phase. The failure was due to the fact that the Gate-Emitter PD would have only been 0.6 V. As a result, when the PIC activated this transistor, 23.4 V was encountered on the PIC output resulting in a cascading failure. A solution to this problem would be to change the top level Darlington Pairs to pnp type modules and control the base of these via additional npn transistors.

Another problem encountered during testing was that the 20 A of current flowing into the motor was not sufficient. This resulted in currents in excess of 25 mA drawn from the PIC thus damaging it further. After much deliberation, it was realised that the only way to get such a circuit to work was to connect many transistors in a Darlington fashion in order to “step up” the current progressively. However, such a design would be expensive and time consuming to build. A more elegant approach was called for.

A MOSFET Starter Circuit

After discussion with various sources [30, 31] and personal research into the operation of FET technology [32], it was decided that the use of MOSFETs in place of Darlington pair transistors would simplify the design of the 3 phase starter circuit. Put simply, a MOSFET will allow a current to flow between the Drain and the Source terminals depending on the level of

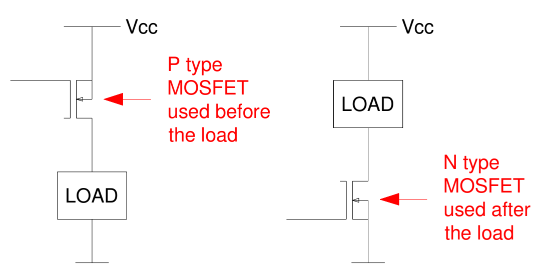

Figure 6.23: Situations to use p and n type MOSFETS

voltage placed on the gate. They have the advantage over transistors that no current flows between the gate and source terminals. Similarly to transistors, MOSFETS come in two types. Depending on whether the load is before or after the MOSFET will determine which type to use. This is shown in figure 6.23.

As discussed at the beginning of section 6.6, when the motor is running, a back e.m.f will be generated. This may be significant enough to damage the MOSFETs and so it was recommended [30] to use reversed diodes to “soak up” these induction spikes.

The risk that both top and bottom gates could be opened allowing a short circuit is greater here due to the transition times for the MOSFET to change state. Therefore, the PIC was programmed with a delay between cutting of one MOSFET and activating the other. However, relying on software to prevent this is also risky. The addition of a diode between the gate of the lower and upper Power MOSFETs electronically prevents both from being active. A full circuit diagram of this arrangement can be found in Appendix 12 with the final construction in figure 6.24.

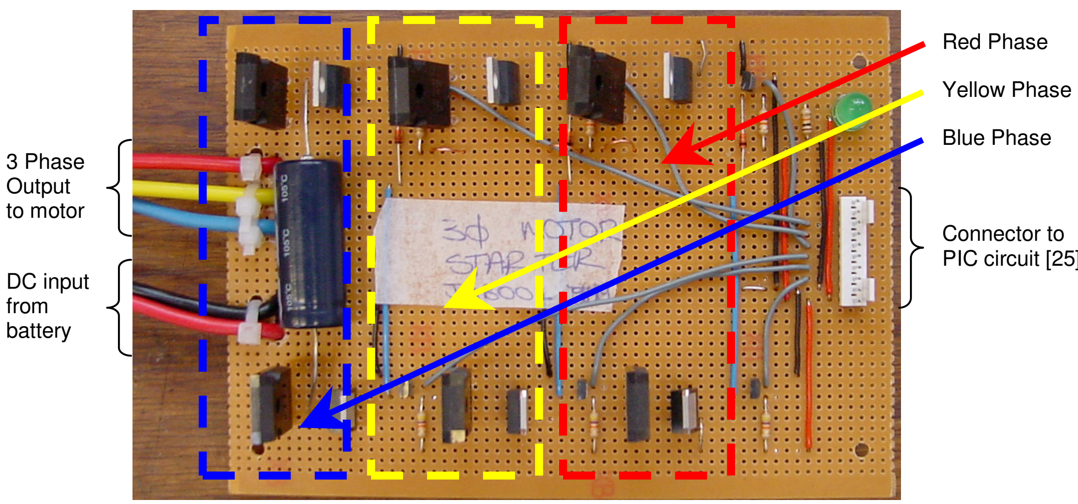

Figure 6.24: Final MOSFET starter circuit

According to the manufacturer’s specifications of all the MOSFETs used, the greatest transition time to achieve change of state was 150 ns. It should have been possible to achieve significant motor speeds using this circuit. In reality the circuitry did allow rotation but only at extremely slow speeds. When the frequency of the signals from the PIC was increased, the motor stopped. After various investigations and debugging efforts, this circuit was abandoned owing to time constraints.

Using a Schulze 32.55 speed controller for starting

During the design of the MOSFET starter circuit, it was realised that it may be possible to use a Schulze 32.55 speed controller safely for this purpose. Such a controller will have to be able to cope with the back e.m.f. from the motor. It is likely that this will be achieved in the same way as for the

MOSFET circuit with reversed diodes across the internal components. This theory is strengthened by the statement in the user documentation [27] indicating that it is important to observe correct DC polarity of the controller. In the event of incorrect connection, a short circuit will occur as a consequence of these diodes.

With the problems incurred by the MOSFET circuit, and time constraints, it was decided to use one of these controllers to simply see if the genset engine would start. This was tried on the configuration as illustrated in figure 6.20 with no load attached to the generator and was successful. Once the engine started, the speed controller was immediately turned off and disconnected to avoid damage. In examining this after the test, no damage had been incurred by the speed controller and it was decided to use this to start the final genset.

6.9.3 Genset Construction

Appendix 13 illustrates the testing proposal for the genset which was agreed by the group at a meeting. Testing the genset required the output of the generator to be connected to a load resistance equivalent to that of the platform. If the genset could provide enough power at this load level, then the test would be successful. When providing 1 kg of thrust, the perimeter fans require a total of 1.6 kW. When running at 30 V, the load resistance needed to be close to ½ Ω in order to match the current demands of the platform. However, no resistor blocks which could handle in excess of 10 A were able to be sourced. Therefore, construction of a load circuit using resistance wire was initiated. The circuit was mounted on a piece of board and was aimed at supporting the resistance wire whilst allowing any connections or adjustments to be made easily and safely. The plans for this board are shown in Appendix 14. This test board offered the following additional advantages:

- The resistance wire was mounted to the back of the board in a regular fashion allowing air to circulate around it when in operation.
- During testing, the board could be mounted beside the genset to act as a protective barrier in the event of engine failure.
- The load resistance was initially set to 5 Ω. This could be unplugged via a banana plug on the front of the board to allow the genset to be tested with no load. Once the 5 Ω load was connected, subsequent connections allowed this to be reduced further until a load typical to that of the platform could be achieved.
- Easy disconnection the speed controller once the engine had started was made possible through connectors on the front of the board.

6.9.4 Initial Genset Testing

Once the load circuit board was developed, testing begun on the Genset. However, it was not possible to collect any results owing to various problems with the connection between the engine and the coupling. As seen in figure 6.20 the coupling was attached to the engine shaft by means of an adaptor. As the motor shaft was threaded, this adapter was made to screw on. When the engine runs in a normal clockwise direction, the adaptor is constantly being tightened. However, when the motor tries to turn the engine in this direction, the adaptor is loosened. Therefore the adaptor was drilled and secured to the motor shaft by grub screws.

Once this issue was rectified, testing was soon aborted again when the flexible coupling failed. A high strength coupling was bought to cope with the initial torque but this failed when the generator became loose from its fixings as a result of excessive vibrations from the engine.

On the next occasion, the entire IC engine failed catastrophically for no obvious reason. It is discussed in R. Holbrook's report [13] that this may have been due to the cumulative marginal misalignments incurred during previous repairs.

6.9.5 Final Genset Testing

In light of this failure, a new OS IC engine was purchased. This was a marine version with an integral flywheel and a water cooled head. At this stage of the project, it was agreed that the genset will not be put on the platform this year and merely tested in order to determine its characteristics. After several months of attempted testing, some results were finally achieved. They are shown in Appendix 15.

6.10 Power Distribution System

During the course of the project, it was unknown if the genset would be capable of providing enough electrical power to satisfy the requirements of the platform. Nonetheless, what ever source is used to provide power, it will still need to be converted into the various levels required by the onboard electronic components. However, for the benefit of the design, it was assumed that the source PD would be 36 V. This PD was chosen as it is the greatest PD which the speed controllers of the perimeter fans will accept. For the same power, the greater the input voltage; the lower the current drawn.

Every electronic sub-system required a DC power supply including the fans. This was achieved by using the rectifier described in the previous section. However, the specific voltage requirements needed to be determined and supplied via a separate power supply circuit. In order to minimise the number of components used, and ultimately the overall weight, the designers of each circuit worked closely to try and use similar voltages. Table 6.5 shows the specific electronic sub-systems with their individual voltage and power requirements.

Electronic sub-system	Requirements
Perimeter Fans	Voltage: 12-36V, Ground Power: 1.6kW
Servo motors for engine throttles	Voltage: 5V, Ground Power: 2.5W
IMU	Voltage: 8V, Ground Power: 12W
IMU Decoder	Voltage: ±15V, 5V, Ground Power: 6W
Control	Voltage: ±15V, Ground Power: 25W
Radio Controlled Receiver	Voltage: ±12V, Ground Power: 25W (allocated)

Table 6.5: Voltage requirements from each electronic sub-system.

It can be seen that both positive and negative voltages are required. Therefore the 36 V supply is needed to be divided in two with the ground reference point set at 18 V. In reality the DC output from the rectifier is actually ±18 V with respect to the three phase supply which simplifies this issue. From the theory on 3 phase power generation in section 6.7 it was shown from phasor diagrams that the sum of all three phases is zero. Therefore using a voltage summer in conjunction with the rectifier will produce the 0V line.

The power supply for all sub-systems, with the exception of the perimeter fans, had the three input voltages of ±18V and 0V. Voltage regulators were used to adjust these to the levels required in table 6.5. LM317 and LM337 regulators were used for positive and negative voltage outputs respectively.

These were chosen as their output voltage could be adjusted via an external feedback circuit. It also proved more cost effective to buy these in quantity rather than individual ones for specific needs. The final design can be seen in figure 6.25. The switches were added for testing purposes only allowing each voltage supply to be isolated if necessary. In application, the switches could be removed to keep weight to a minimum. The circuit diagram can be seen in Appendix 16.

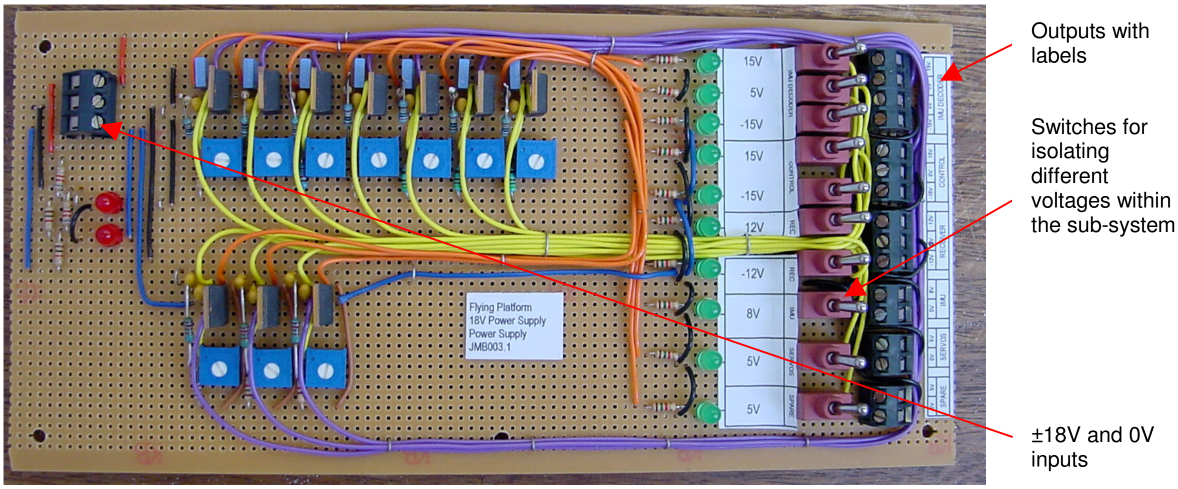

Figure 6.25: Platform power supply with isolation switches for testing purposes only

The motors for the perimeter fans were powered directly from the rectifier. These motors were specified to accept any voltage between 12 and 36V. As already explained, in order to conserve current, the higher voltage level was chosen.

Testing of Power Supply

At the time of writing, the genset was not able to be tested with the power supply unit. Therefore, a ±18V bench power supply was used. According to the data sheet on the LM317 voltage regulators, no more than 0.5 A should be drawn from the 5 V lines. This can be seen from the data sheet in Appendix 17. Therefore, a 20 Ω resistor was used and the voltage across this was calibrated to 5 V. For the +8 V, +12 V and +15 V lines the maximum rated current was 2.2 A. Therefore these outputs were calibrated using a 10 ohm load resistance.
The LM337 voltage regulators behaved in the same way as the LM317s but with the only difference that they could handle negative voltages. Therefore, they were able to be calibrated and tested using the same method as before.

7. Discussion Conclusion and Future Recommendations

This report has discussed that Design and Development of the electrical aspect of the Flying Platform from work conducted by the author. It was unfortunate that the platform could not achieve tethered flight in a similar fashion to the previous group but this was mainly due to the high number of problems and failures occurred during the course of the project. However, achievements have been made in the exploration of the concepts detailed in the aims. These are discussed in the following sections.

Genset

After several problems, the genset was eventually testing and results were obtained. Although, results are limited, initial observations look promising and this concept may be a viable solution to power supply requirements on the platform. As explained in the theory, three phase power generation is the only way to obtain as much power from as little weight as possible. When the project is continued in October 2004, it is hoped that further testing of the genset will continue in order to explore its full potential.

Power Supply

A power supply unit has been designed, built and tested. This will satisfy the requirements of all the electronic sub modules on the platform. As explained in the text, this design is for test purposes only. In order to conserve weight, this unit will need to be reduced before it can be mounted on the platform.

Propulsion

Owing to a lack of structure, it was not possible to determine whether the total thrust generated from the larger central duct and four perimeter fans will be enough to lift two IC engines and a generator. This is recommended to be the starting point for any continued development. If this configuration is proved to work, then the Platform is closer to flight. However, if it will not work, then other methods must be explored.

Appendix 1: The Product Design Specification (PDS)

Performance	1. Must hover approx. 1 m above the ground. 2. Flight Duration to be approx. 20 minutes. 3. Must remain stable 4. Must provide viable operating platform 5. Must be able to carry a payload of up to 3 kg. 6. Must have the capability to have the ON/OFF controlled by remote.
Environment	1. Must be capable of operating in a temperature range of -10℃ to 50℃. 2. Must be capable of operating in humid conditions and to be water resistant when operating in light rain. 3. Must be operated in minimal air flow disturbances, i.e. minimal wind speeds.
Maintenance	1. Onboard battery must be easily accessible for possible replacement and recharging. 2. Fuel tank for internal combustion engine must also be easily accessible for refuelling.
Life in Service	1. Product's life service is to be approx. 5 years.
Target production cost	1. A budget of £1000 has been assigned to the project.
Size	1. The Flying Platform's dimensions to be similar to the dimensions specified in the previous group's report.
Weight	1. Yet to be determined but should be designed for minimum weight possible. Estimated weight including payload is 10 kg.
Materials	1. Materials used must have a high mechanical tolerance and must have as low a density as possible.
Design Constraints	1. The flight must be completely autonomous. 2. The design must not be a helicopter design. 3. Must use an onboard IC engine for power generation.

Appendix 2: The 6 Degrees of Freedom

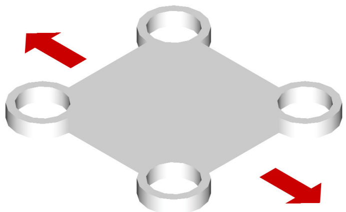

1. Forward / Reverse

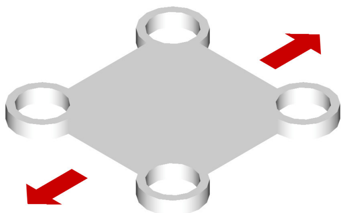

2. Left / Right

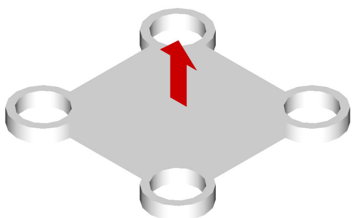

3. Up / Down

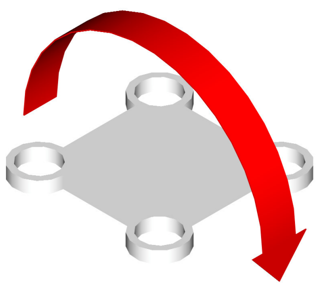

4. Pitch

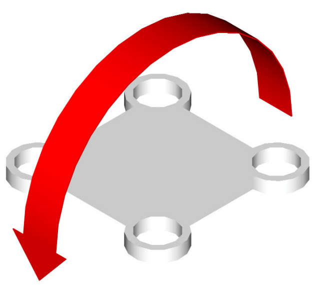

5. Roll

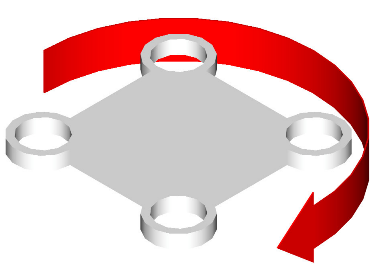

6. Yaw

Appendix 3: A copy of the Minutes for a meeting

UNIVERSITY of EXETER

Fourth Year Group Project
FLYING PLATFORM

Minutes

Date: 16/10/2003
Room: 101
Meeting: 2

Group Members		**Present**	**Apologies**
Liam Dushynsky	LD	✓	
Richard Forder	RF	✓	
Richard Holbrook	RH	✓	
Rebecca Hughes	RCH	✓	
Kevin Lowis	KL	✓	
James Mackenzie-Burrows	JMB	✓	
Jody Muelaner	JM	✓	
Chris Poczka	CP	✓	
Alex Tombling	AT	✓	
Guests			
Dr. Martin Jenkins	MAJ	✓	
Dr. Garry Lester	GAL		✓

2.1 Apologies

Apologies were received by MAJ on behalf of GAL as he is currently attending a conference abroad.

2.2 Previous Minutes

The minutes from Meeting 1 on 13/10/2003 were accepted by all.

2.3 Previous Matters:

A regular formal meeting time was agreed by all for every Thursday at 10am with MAJ & GAL.

2.4 Matters Discussed:

MAJ used this meeting to demonstrate the current platform and to advise the group how to undertake the project.

2.4.1 Project Management:

- Minutes are taken as legal insurance and are proof of any decisions that are made. They must be taken at meetings where important decisions are made. A copy of the minutes must be issued to the whole group ASAP.

- An agenda must be issued at the beginning of meetings with a logical numbering system to enable easy tracking. This numbering system will then be used in the resulting minutes.

- Deadlines of tasks must be thought through carefully. Fridays were advised to be poor deadlines as no work is then completed over the weekend.

- The idea of a website resource system was agreed to be a good idea but a warning was issued: it must not take long to set up and maintain.

2.4.2 Demonstration of the Current Platform:

Problems:

- Response times of gyros are a little slow resulting in instability.

- Platform needs an umbilical to provide power as batteries last barely a minute. This no longer makes the platform autonomous.

- Digital circuitry cannot be used as they have slower response times than analogue

Requirements:

- An internal combustion (IC) engine is to be used to produce electricity via a generator.

- The electricity produced will charge the batteries which supply the fans.

- A central fan is required to work in conjunction with the outer four to provide lift. The outer four with then control the stability.

Product Design Specification (PDS):

- Flight Time = 20 minutes (approx.)
- Payload = up to 5kg
- Dimensions = fixed
- The current frame must not be changed except in the centre to accommodate the IC engine and central fan.
- Height of flight = 1m (approx.)
- Pitch = stabilised
- Roll = stabilised
- Yaw = Not a necessary concern at the moment.
- Must have a remote ON/OFF control. This must be the only external control.

2.5 Task List:

Task	Action	Deadline
Arrange possible meeting times with GAL	JMB	21/10/2003
Further Reading of Reports	ALL	20/10/2003

2.6 General Notices:

None taken.

2.7 Budget:

Not discussed.

2.8 Next Meeting:

The next group only meeting with be at **10:00am** on **Monday 20/10/2003** in **Room 102A.**

Appendix 4: A Block Diagram of the Platform Components

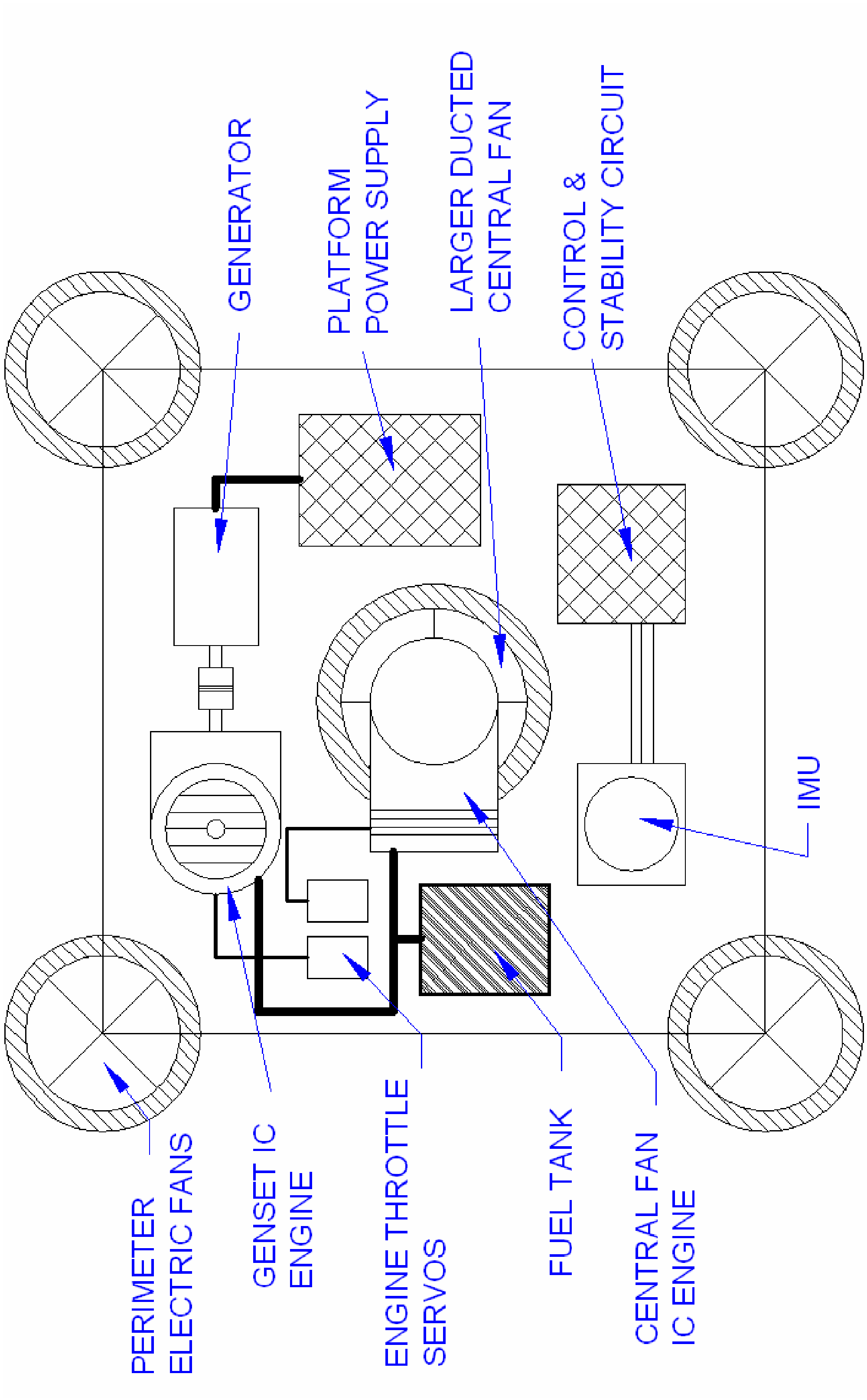

Appendix 5: Results from Initial Thrust Testing

Pulse Width (ms)	Voltage Output (V)	Frequency (Hz)	RPS	RPM	Current In (A)	Voltage In (V)	Power In (W)	Mass Reading (g)	Thrust (g)
1.00	0	0	0	0	0	25.4	0	0	0.00
1.07	0.72	480	80	4800	0.4	25.3	10.12	90	90.00
1.10	0.74	493.333333	82.222	4933.3	0.5	25.2	12.6	90	45.45
1.15	1.05	700	116.67	7000	1	25.1	25.1	185	93.42
1.20	1.33	886.666667	147.78	8866.7	1.8	25	45	325	164.11
1.25	1.57	1046.66667	174.44	10467	2.7	24.9	67.23	455	229.75
1.30	1.8	1200	200	12000	3.6	24.8	89.28	630	318.12
1.35	2.04	1360	226.67	13600	4.8	24.7	118.56	765	386.29
1.40	2.23	1486.66667	247.78	14867	6.8	24.6	167.28	945	477.18
1.45	2.5	1666.66667	277.78	16667	9	24.5	220.5	1200	605.94
1.50	2.77	1846.66667	307.78	18467	10.5	24.5	257.25	1420	717.03
1.55	2.97	1980	330	19800	13.3	24.3	323.19	1700	858.42
1.60	3.24	2160	360	21600	16.8	24.3	408.24	2000	1009.90
1.65	3.46	2306.66667	384.44	23067	20	24.3	486	2300	1161.39
1.70	3.7	2466.66667	411.11	24667	24.1	24.1	580.81	2620	1322.97
1.75	3.89	2593.33333	432.22	25933	28	24	672	2925	1476.98
1.80	4.1	2733.33333	455.56	27333	34	23.9	812.6	3280	1656.24
1.85	4.31	2873.33333	478.89	28733	39	23.8	928.2	3600	1817.82
1.90	4.48	2986.66667	497.78	29867	46	23.7	1090.2	3930	1984.46
1.95	4.57	3046.66667	507.78	30467	48	23.7	1137.6	4120	2080.40
2.00	4.58	3053.33333	508.89	30533	48.8	23.7	1156.56	4120	2080.40

Appendix 5: Results from Initial Thrust Testing (ctd.)

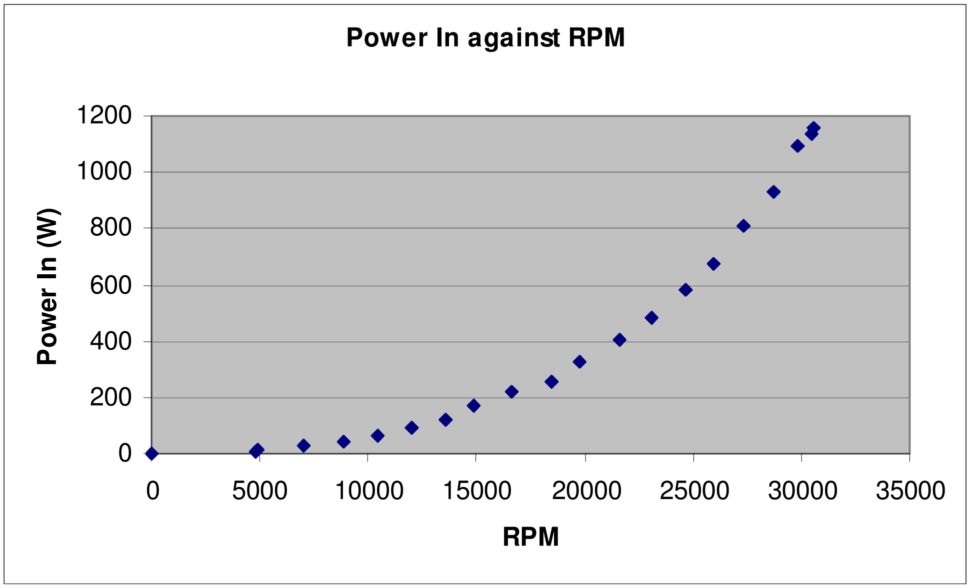

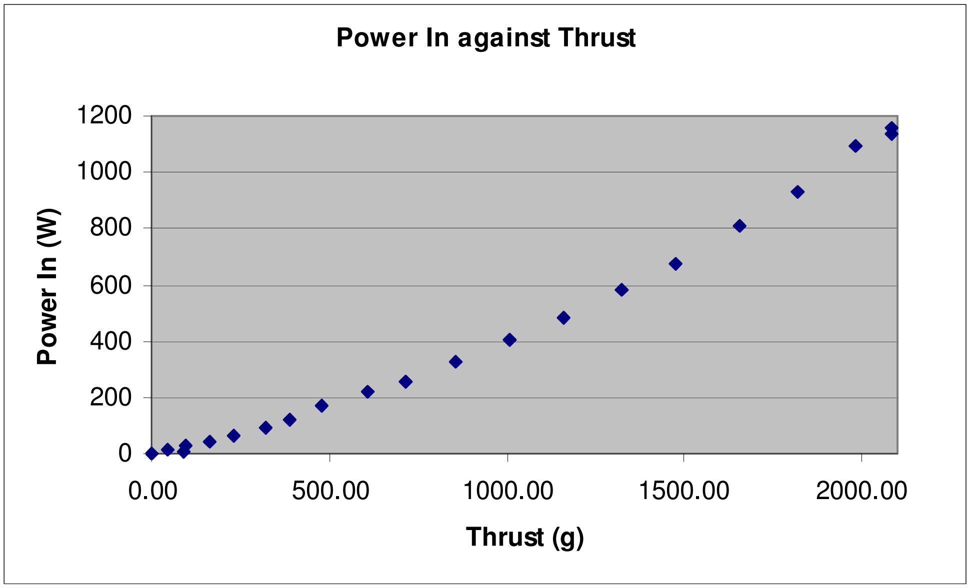

Appendix 6: Group Summary of Ultra Capacitors

UNIVERSITY of EXETER

Fourth Year Group Project

FLYING PLATFORM

Power Systems

UltraCapacitors

Another way to store electrical energy other than in a battery is by using a capacitor. However, in situations where high power demands are necessary, capacitors in the Farad region are necessary. Such capacitors used to be impractically large but recently, they have been reduced to a much smaller scale resulting in – UltraCapacitors.

Currently, there are only 2 main manufacturers of UltraCapicitors – Maxwell Technologies, and Tavrima. Coupled with the fact that they are a new product means that they are not widely commercially available. Suggested applications by the manufacturers include hybrid electric vehicles.

UltraCapacitors compare to Lead Acid batteries as follows:

	Lead Acid	**UltraCapacitor**
Charge Time	1 – 5hrs	0.3 – 30s
Discharge Time	0.3 – 3hrs	0.3 – 30s
Energy (Wh/kg)	10 – 100	1 – 10
Cycle Life	1000	>500,000
Specific Power (W/kg)	<1000	<10,000
Efficiency	70% - 85%	85% - 98%

The following list of current UltraCapacitors gives an idea of the types of values associated with them.

Manufacturer	**Prod. Code**	**Capacitance**	**Output P.D.**	**Max I**	**Weight**
Maxwell	BCAP0013	450F	2.5	180A	190g
Maxwell	BCAP0014	900F	2.5	250A	260g
Maxwell	PC100E	100F	2.5	25A	37g
Maxwell	PC2500	2.7kF	2.5	625A	725g
Tavrima	ESCAP10/42	11F	42	62A	10.5kg
Tavrima	ESCAP 2/10	12F	18	460A	9.5kg

Appendix 7: Results from Plettenberg HP220 Testing

V in (V)	I in (A)	Electrical Power In (W)	Strobe Reading	Speed (rpm)	V out (V)	R load (?)	I out (A)	Electrical Power Out (W)	Efficiency
25.2	0.4	10.08	3000	6000	2.4	5	0.48	1.15	11.43%
25.1	1.3	32.63	6800	13600	7.1	5	1.42	10.08	30.90%
25.0	2.3	57.50	9800	19600	10.9	5.1	2.14	23.30	40.51%
24.9	3.3	82.17	12000	24000	13.4	5.2	2.58	34.53	42.02%
24.8	3.8	94.24	13600	27200	15.4	5.3	2.91	44.75	47.48%
24.7	4.4	108.68	15000	30000	17	5.4	3.15	53.52	49.24%
24.6	5.0	123.00	16000	32000	18.2	5.4	3.37	61.34	49.87%
24.6	5.2	127.92	17000	34000	19.3	5.5	3.51	67.73	52.94%
24.6	6.4	157.44	18600	37200	21.2	5.6	3.79	80.26	50.98%
24.6	6.4	157.44	19000	38000	21.9	5.6	3.91	85.64	54.40%
25.1	2.3	57.73	7900	15800	8.3	4	2.08	17.22	29.83%
24.9	4.5	112.05	13200	26400	14.5	4	3.63	52.56	46.91%
24.7	6.5	160.55	16200	32400	18.3	4	4.58	83.72	52.15%
24.6	8.0	196.80	19000	38000	21.4	4	5.35	114.49	58.18%
25.0	2.3	57.50	7500	15000	7.2	3	2.40	17.28	30.05%
24.8	5.0	124.00	12600	25200	13.6	3	4.53	61.65	49.72%
24.6	7.3	179.58	15000	30000	17.5	3	5.83	102.08	56.85%
24.5	9.5	232.75	18800	37600	21	3	7.00	147.00	63.16%
24.8	2.3	57.04	6800	13600	6.9	2	3.45	23.81	41.73%
24.8	5.4	133.92	11800	23600	12.7	2	6.35	80.65	60.22%
24.6	9.0	221.40	15400	30800	16.7	2	8.35	139.45	62.98%
24.4	11.3	275.72	18800	37600	20.6	2	10.30	212.18	76.95%
25.0	2.3	57.50	5800	11600	5.5	1	5.50	30.25	52.61%
24.7	6.8	167.96	10500	21000	10.9	1	10.90	118.81	70.74%
24.7	12.0	296.40	14600	29200	15.4	1	15.40	237.16	80.01%
24.3	15.9	386.37	18200	36400	19.3	1	19.30	372.49	96.41%

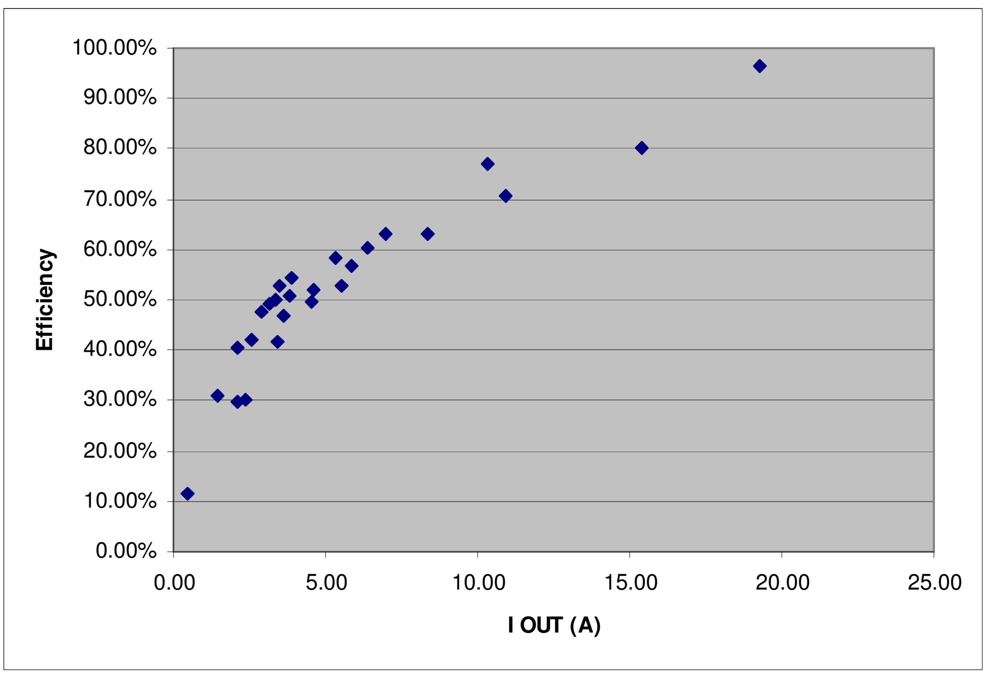

Appendix 8: Results from Graupner 12V Motor Testing

V in (V)	I in (A)	Electrical Power In (W)	Strobe Reading	Speed (rpm)	V out (V)	R load (?)	I out (A)	Electrical Power Out (W)	Efficiency
25.2	0.7	18.14	3300	6600	4	5	0.80	3.20	17.64%
25.1	1.6	40.16	6300	12600	7.7	5	1.54	11.86	29.53%
25.0	2.5	62.50	8700	17400	10.6	5	2.12	22.47	35.96%
25.1	0.6	15.06	3200	6400	4	4	1.00	4.00	26.56%
25.0	1.7	42.50	6100	12200	7.5	4	1.88	14.06	33.09%
24.9	2.6	64.74	8400	16800	10	4	2.50	25.00	38.62%
24.9	3.6	89.64	10000	20000	11.98	4	3.00	35.88	40.03%
25.1	0.7	17.57	3100	6200	3.7	3	1.23	4.56	25.97%
25.0	1.7	42.50	5800	11600	6.9	3	2.30	15.87	37.34%
25.0	2.8	70.00	7800	15600	9.2	3	3.07	28.21	40.30%
24.9	4.0	99.60	8700	17400	11	3	3.67	40.33	40.50%
25.1	0.7	17.57	2600	5200	3	2	1.50	4.50	25.61%
25.0	1.9	47.50	5000	10000	6	2	3.00	18.00	37.89%
25.0	3.0	75.00	7000	14000	7.8	2	3.90	30.42	40.56%
24.9	4.4	109.56	9000	18000	9	2	4.50	40.50	36.97%
25.2	0.5	12.60	1500	3000	1.5	1	1.50	2.25	17.86%
25.1	0.9	22.59	2500	5000	2.3	1	2.30	5.29	23.42%
25.1	1.8	45.18	3400	6800	3.6	1	3.60	12.96	28.69%
25.0	2.4	60.00	4900	9800	4.5	1	4.50	20.25	33.75%
24.9	3.4	84.66	5900	11800	5.6	1	5.60	31.36	37.04%

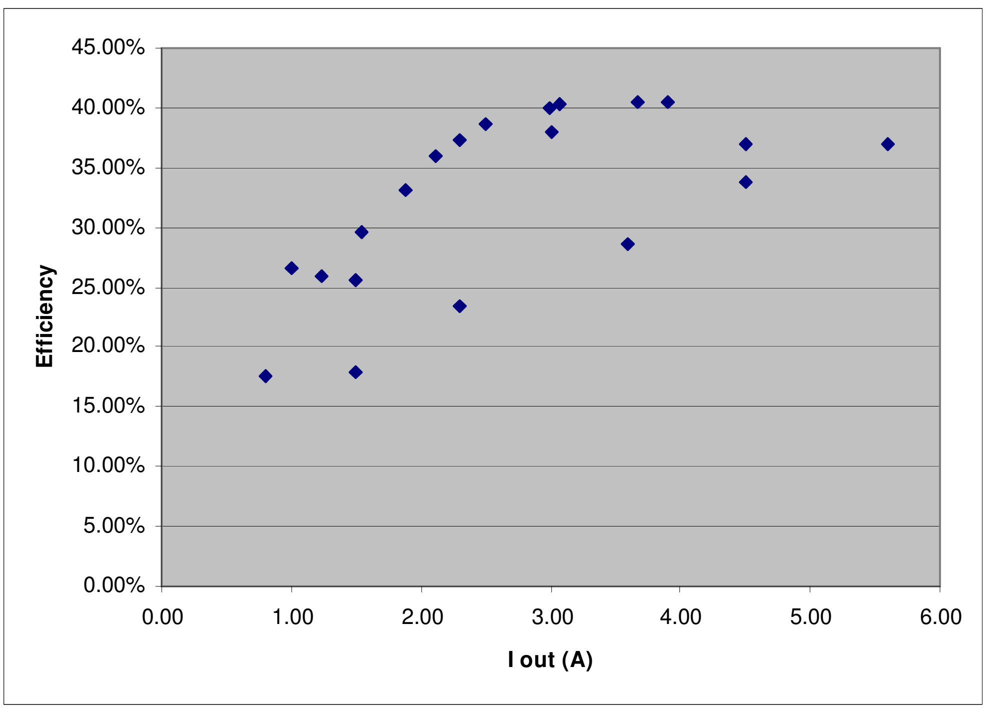

Appendix 9: Results from Plettenberg HP 370 Testing

V in (V)	I in (A)	Electrical Power In (W)	Strobe Reading	Speed (rpm)	V out (V)	R load (?)	I out (A)	Electrical Power Out (W)	Efficiency
25.0	0.4	10.00	12	2400	2.25	5	0.45	1.01	10.13%
24.9	1.9	47.31	30.5	6100	7.48	5	1.50	11.19	23.65%
24.7	4.7	116.09	52	10400	13.81	5	2.76	38.14	32.86%
24.5	7.8	191.10	72	14400	19.34	5	3.87	74.81	39.15%
24.3	11.3	274.59	90.5	18100	24.4	5	4.88	119.07	43.36%
24.1	15.0	361.50	108	21600	29.5	5	5.90	174.05	48.15%
24.0	19.4	465.60	127	25400	34.6	5	6.92	239.43	51.42%
23.9	23.5	561.65	145	29000	39.6	5	7.92	313.63	55.84%
23.8	29.1	692.58	164	32800	44.6	5	8.92	397.83	57.44%
23.8	29.6	704.48	168	33600	45.4	5	9.08	412.23	58.52%
24.9	0.4	9.96	12	2400	2.11	4	0.53	1.11	11.17%
24.8	2.2	54.56	31	6200	7.48	4	1.87	13.99	25.64%
24.6	5.3	130.38	52	10400	13.63	4	3.41	46.44	35.62%
24.4	8.9	217.16	71	14200	18.96	4	4.74	89.87	41.38%
24.3	13.0	315.90	89	17800	24	4	6.00	144.00	45.58%
24.1	17.6	424.16	108	21600	28.9	4	7.23	208.80	49.23%
24.0	22.7	544.80	126	25200	34	4	8.50	289.00	53.05%
23.8	28.4	675.92	143	28600	38.5	4	9.63	370.56	54.82%
23.7	35.1	831.87	162	32400	43.3	4	10.83	468.72	56.35%
23.7	35.8	848.46	164	32800	44.2	4	11.05	488.41	57.56%
25.0	0.6	14.50	9.5	1900	1.69	3	0.56	0.95	6.57%
24.8	3.2	79.36	26	5200	5.94	3	1.98	11.76	14.82%
24.6	8.1	200.24	44	8800	10.84	3	3.61	39.17	19.56%
24.3	14.5	352.35	62	12400	15.5	2.9	5.34	82.84	23.51%
24.1	21.6	520.56	76	15200	19.85	2.8	7.09	140.72	27.03%
23.9	29.8	712.22	92	18400	24	2.7	8.89	213.33	29.95%
23.7	38.8	919.56	106	21200	27.7	2.6	10.65	295.11	32.09%
23.5	47.4	1113.90	128	25600	30.9	2.5	12.36	381.92	34.29%
24.9	0.4	9.96	10	2000	1.7	2	0.85	1.45	14.51%
24.8	3.2	79.36	27.5	5500	6.1	2	3.05	18.61	23.44%
24.6	8.5	209.10	44.5	8900	10.9	2	5.45	59.41	28.41%
24.3	15.2	369.36	61	12200	15.4	1.9	8.11	124.82	33.79%
24.1	22.7	547.07	75.5	15100	19.3	1.8	10.72	206.94	37.83%
23.9	30.8	736.12	88	17600	22.8	1.7	13.41	305.79	41.54%
23.6	69.4	1637.84	105	21000	25.6	1	25.60	655.36	40.01%

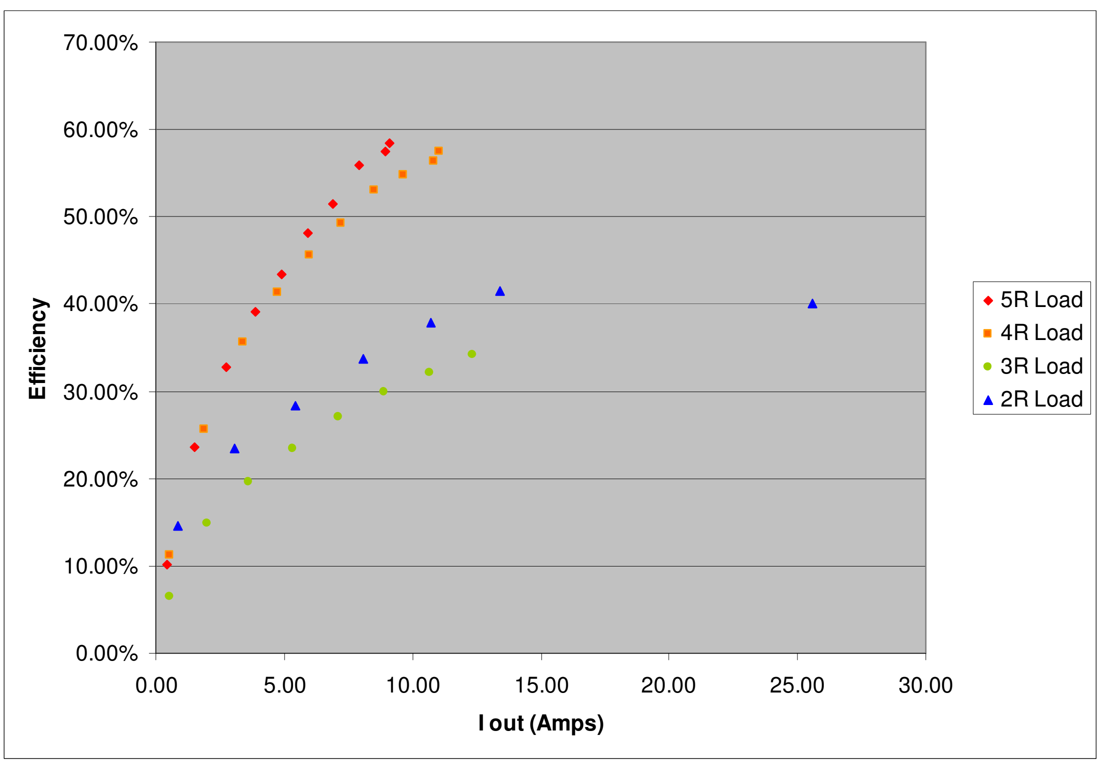

Appendix 10: Block Diagram of Platform Starter System

UNIVERSITY of EXETER

Fourth Year Group Project

FLYING PLATFORM

Electrical Power Systems

Starters

Version 1.0
12/02/2004

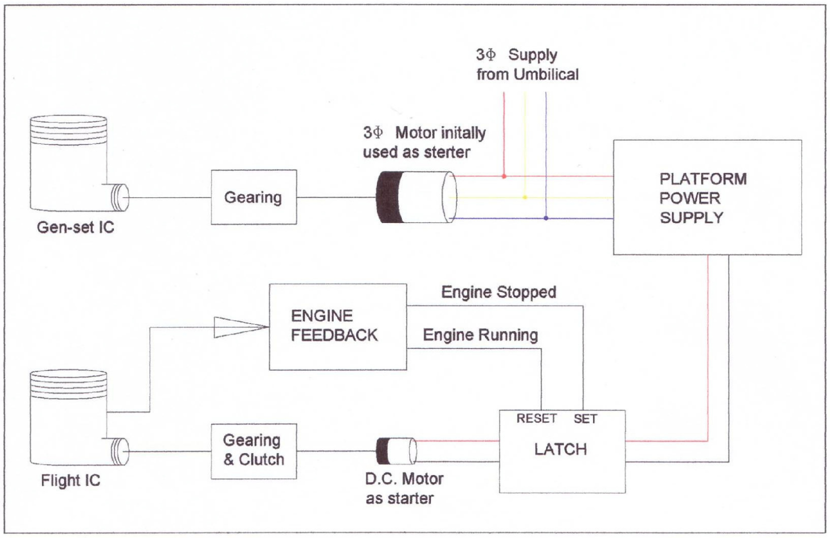

Start up Process

- Umbilical is attached to the platform supplying 3 phase.
- This supply is protected with an RCD which will trip as soon as it detects any generated reverse current. This will occur when the engine has started and is trying to for current back down the umbilical.
- As soon as the on board power supply is established, the feedback circuit from the flight IC will detect that it is not running and will set the latch.
- This will engage the D.C. motor to the IC through the clutch.
- Once the engine has started, the feedback circuit will detect this and reset the latch, switching off the D.C. motor.
- The platform is ready for flight.

In flight restart of Flight IC

Using the on board power supply to start up the flight IC initially will also allow this to be done in flight through the feedback and latch system.

Appendix 11: Circuit Diagram of Darlington Pair 3 Phase Motor Circuit (Circuit No: jmb001)

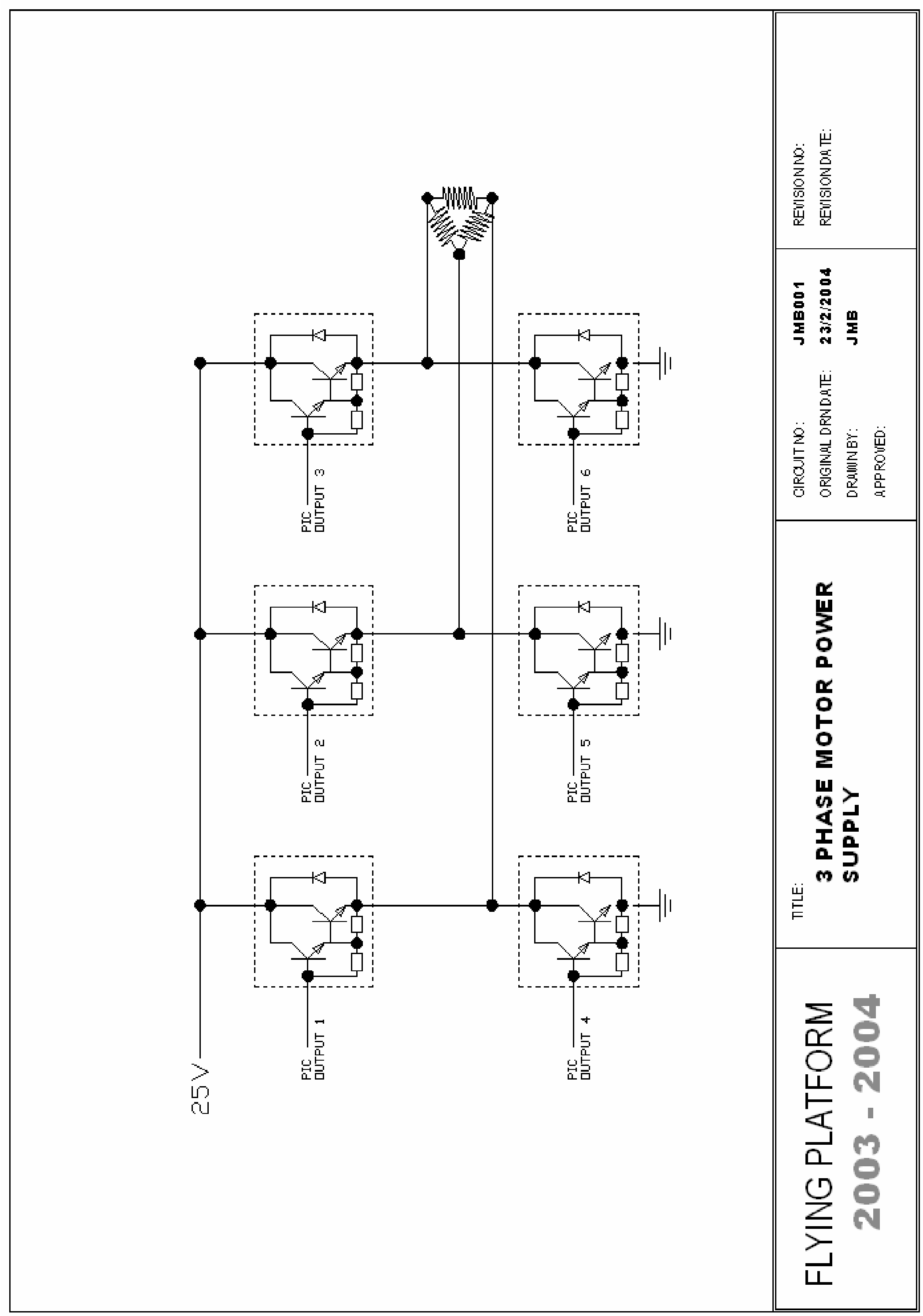

Appendix 12: Circuit Diagram of MOSFET 3 Phase Motor Circuit (Circuit No: jmb002)

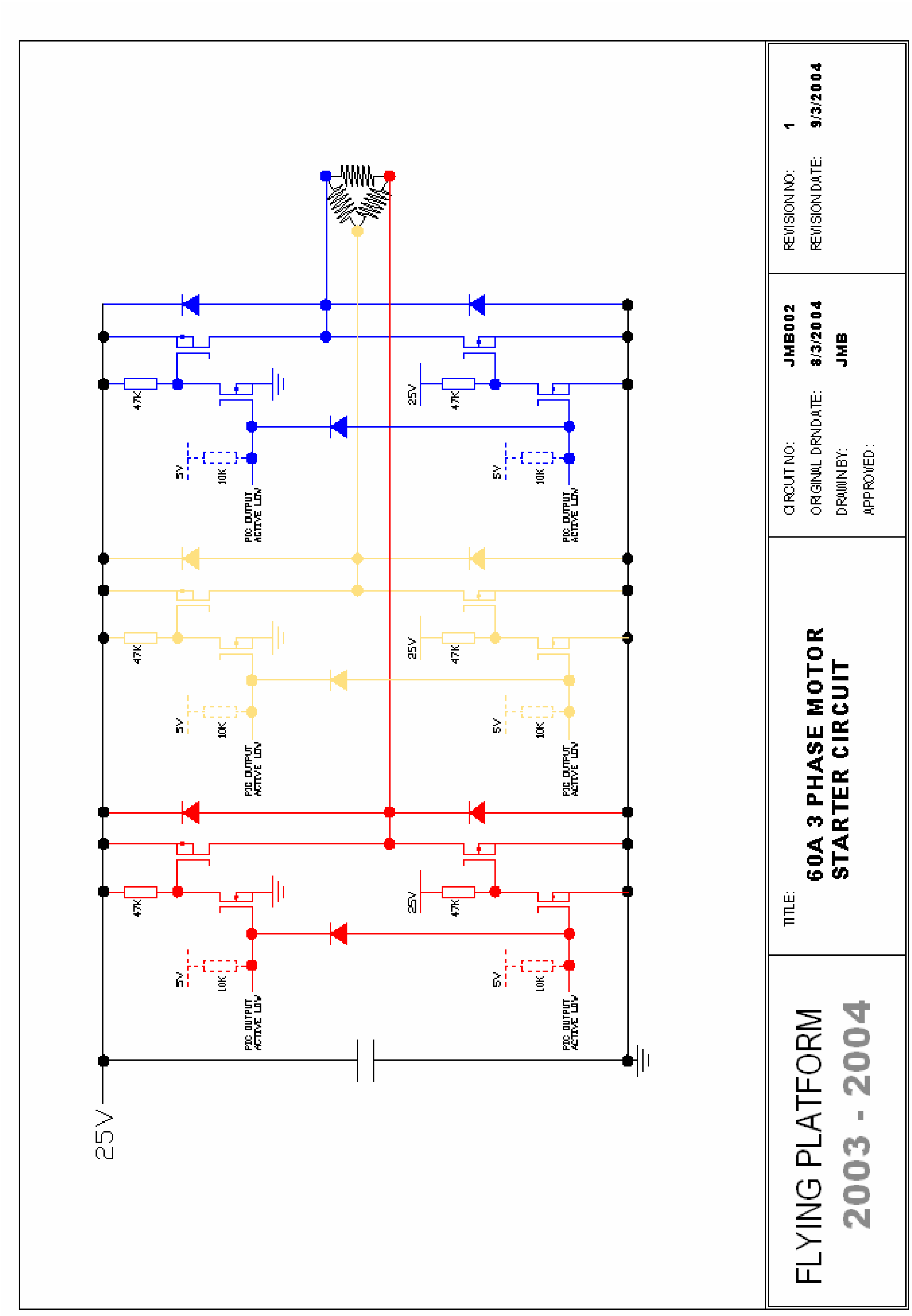

Appendix 13: Procedure for Testing Genset

UNIVERSITY of EXETER

Fourth Year Group Project

FLYING PLATFORM

Electrical Power Systems

Genset Test Proceedure

Version 1.0
19/02/2004

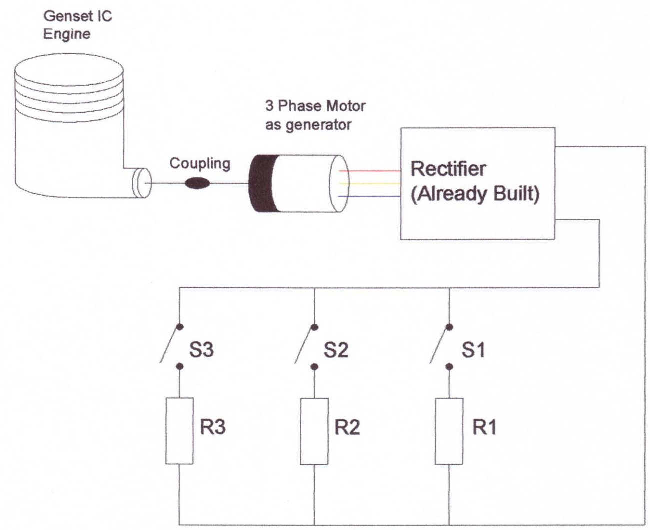

Genset Test Circuit

The circuit above is used to test the effects of sudden loading on the genset IC (i.e. the effect of a severe step input into the stability of the flying platform).

R1 = Resistance to match worst case scenario lowest load. This would occur when the platform is too high and starts to descend. The current demand in this case will be low.

R2 = Combined with R1, this will equate to the load of the platform when it is in perfect stability.

R3 = Combined with R1 and R2, this will mimic the effect of a worst case scenario step input in the stability of the platform requiring the most current draw.

The effect of switching between these loads should make it possible to see the effects on the IC. The aim is to ensure that the engine will not become overloaded and suddenly stop as a direct result of a disturbance.

Appendix 14: Genset Test Board

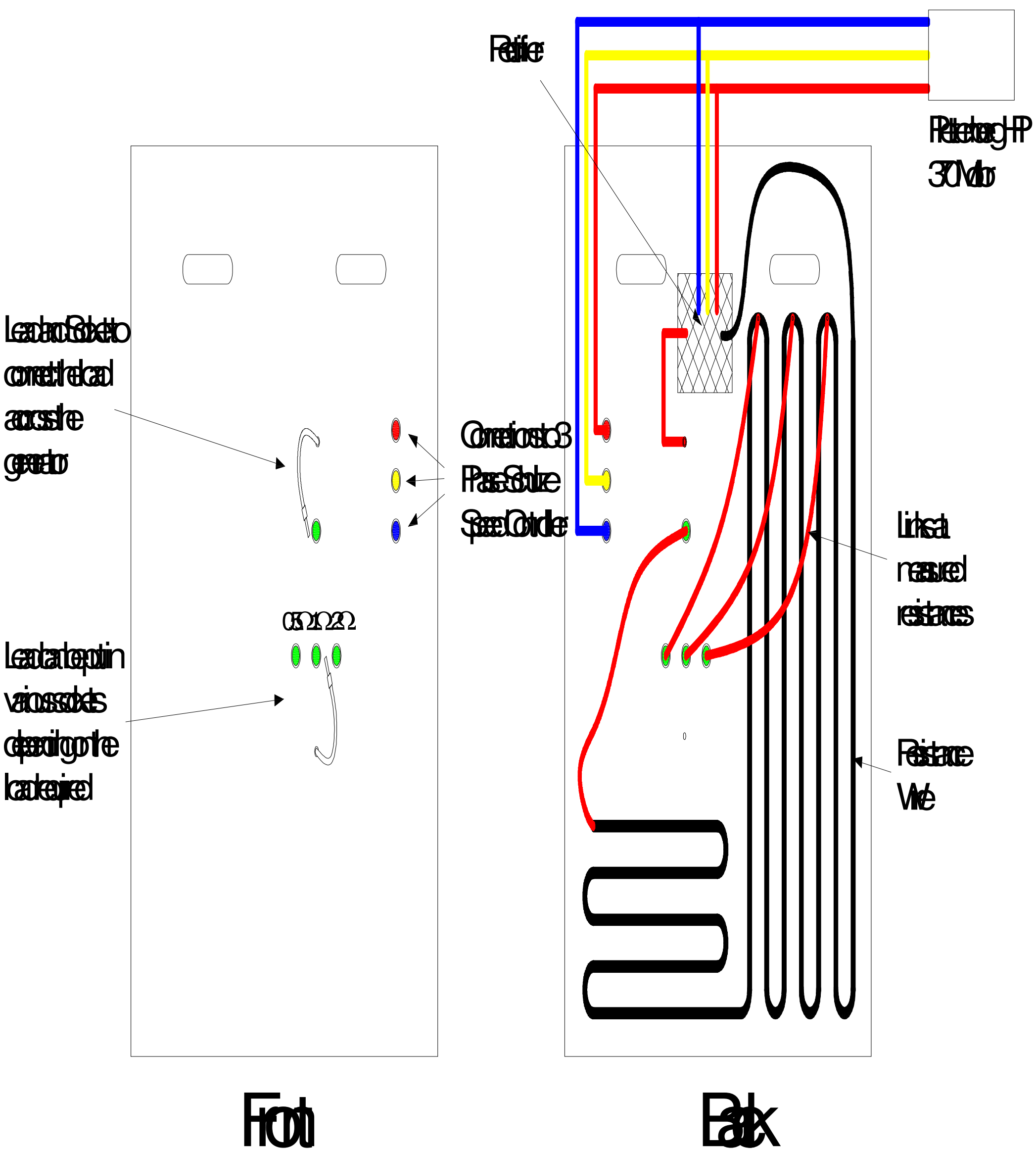

Appendix 15: Genset Test Results

Strobe Reading	Speed (±100) (rpm)	Load Resistance (?)	V out (V)	I out (A)	Electrical Power Out (W)	Integrity of result
155	15500	0.5	18.0	36.0	648.00	Good
160	16000	0.5	18.5	37.0	684.50	Good
182	18200	0.5	22.0	44.0	968.00	Good
185	18500	0.5	20.0	40.0	800.00	Good
190	19000	0.5	21.9	43.8	959.22	Good
190	19000	0.5	22.0	44.0	968.00	Good
210	21000	0.5	24.0	48.0	1152.00	Good
180	18000	1.0	2.4	2.4	5.76	Poor
150	15000	5.0	20.7	4.1	85.70	Good
183	18300	5.0	25.0	5.0	125.00	Good
170	17000	Open Circuit	30.0	0.0	0.00	Good
190	19000	Open Circuit	33.0	0.0	0.00	Good

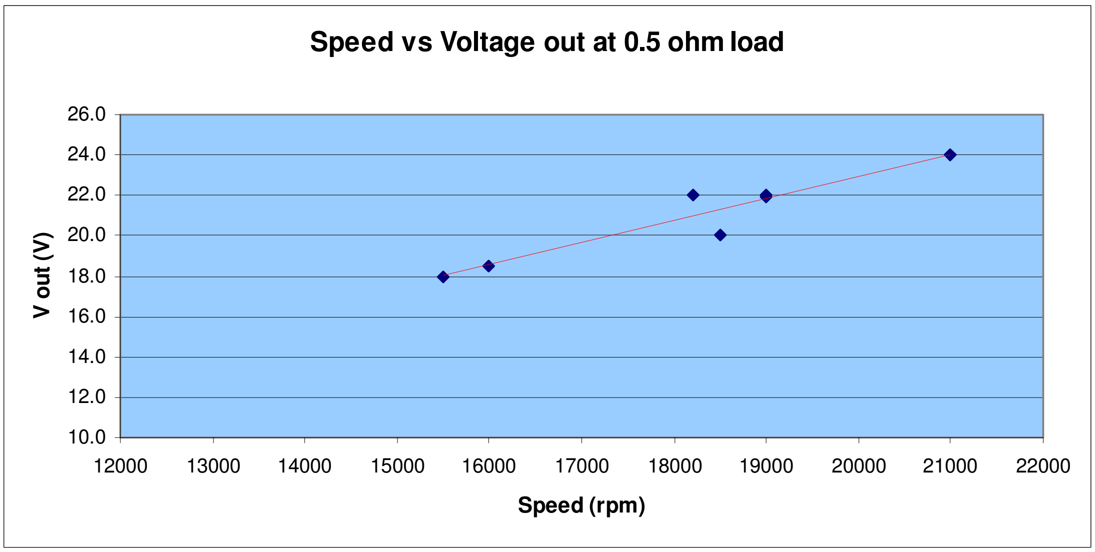

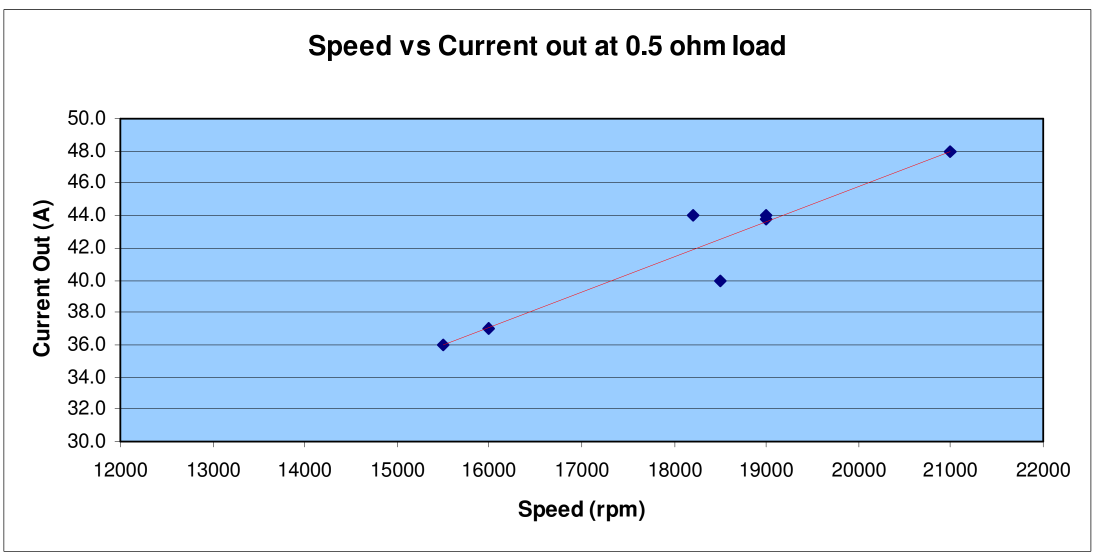

Appendix 16: Platform Power Supply Circuit

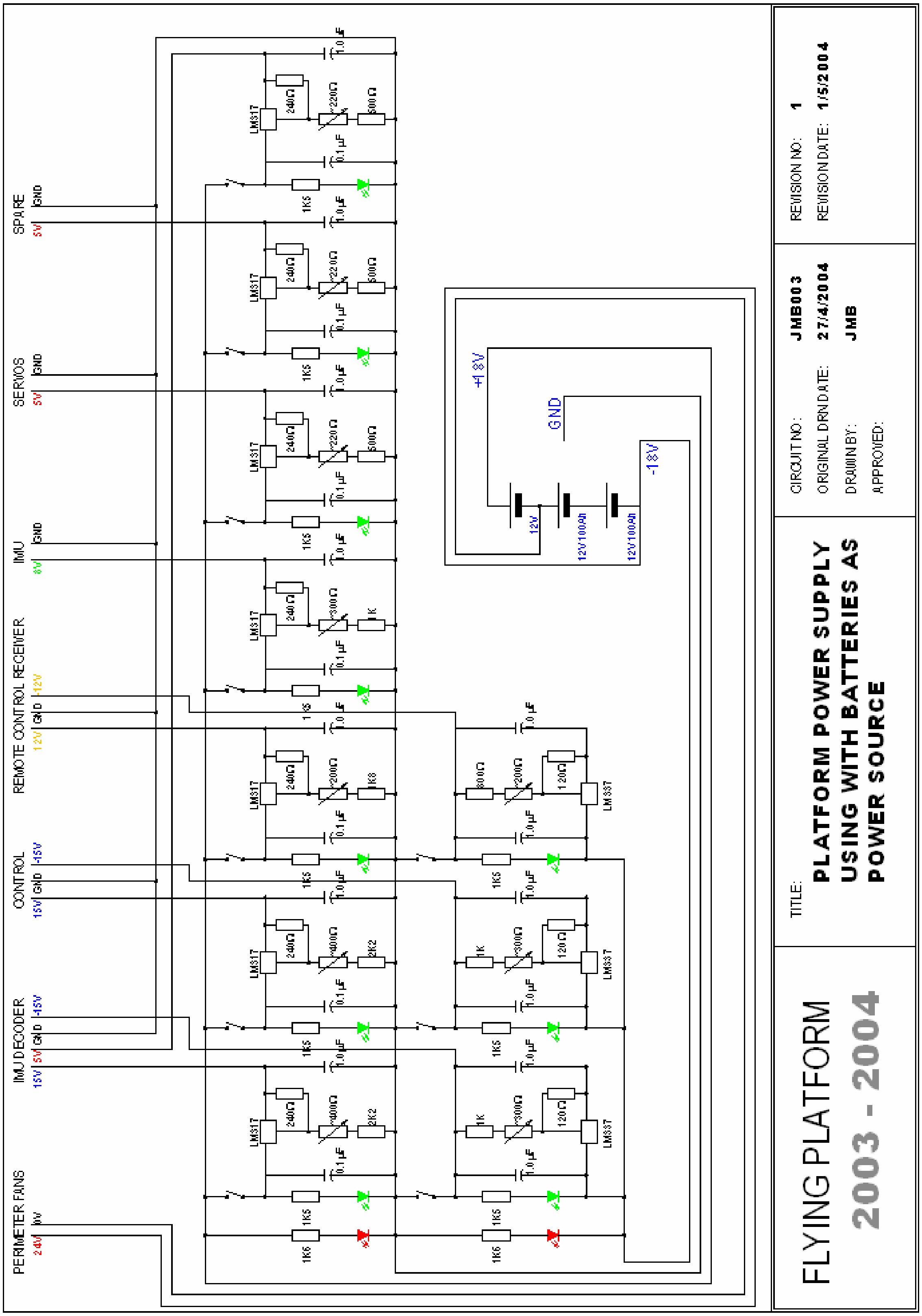

Appendix 17: Copy of LM317 Voltage Regulator Data Sheet

ON Semiconductor™

Three-Terminal Adjustable Output Positive Voltage Regulator

The LM317 is an adjustable 3–terminal positive voltage regulator capable of supplying in excess of 1.5 A over an output voltage range of 1.2 V to 37 V. This voltage regulator is exceptionally easy to use and requires only two external resistors to set the output voltage. Further, it employs internal current limiting, thermal shutdown and safe area compensation, making it essentially blow–out proof.

The LM317 serves a wide variety of applications including local, on card regulation. This device can also be used to make a programmable output regulator, or by connecting a fixed resistor between the adjustment and output, the LM317 can be used as a precision current regulator.

- Output Current in Excess of 1.5 A
- Output Adjustable between 1.2 V and 37 V
- Internal Thermal Overload Protection
- Internal Short Circuit Current Limiting Constant with Temperature
- Output Transistor Safe–Area Compensation
- Floating Operation for High Voltage Applications
- Available in Surface Mount D^2PAK, and Standard 3–Lead Transistor Package
- Eliminates Stocking many Fixed Voltages

LM317

THREE–TERMINAL ADJUSTABLE POSITIVE VOLTAGE REGULATOR

SEMICONDUCTOR TECHNICAL DATA

T SUFFIX
PLASTIC PACKAGE
CASE 221A

Heatsink surface connected to Pin 2.

Pin 1. Adjust
2. V_{out}
3. V_{in}

D2T SUFFIX
PLASTIC PACKAGE
CASE 936
(D^2PAK)

Heatsink surface (shown as terminal 4 in case outline drawing) is connected to Pin 2.

Standard Application

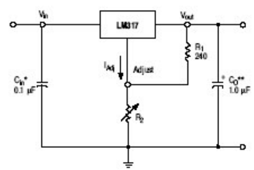

* C_{in} is required if regulator is located an appreciable distance from power supply filter.
** C_O is not needed for stability, however, it does improve transient response.

$$V_{out} = 1.25\,V\left(1 + \frac{R_2}{R_1}\right) + I_{Adj}\,R_2$$

Since I_{Adj} is controlled to less than 100 µA, the error associated with this term is negligible in most applications.

ORDERING INFORMATION

Device	Operating Temperature Range	Package
LM317BD2T	T_J = –40° to +125°C	Surface Mount
LM317BT		Insertion Mount
LM317D2T	T_J = 0° to +125°C	Surface Mount
LM317T		Insertion Mount

March, 2001 – Rev. 2   1   Publication Order Number: LM317/D

LM317

MAXIMUM RATINGS

Rating	Symbol	Value	Unit
Input–Output Voltage Differential	$V_I–V_O$	40	Vdc
Power Dissipation Case 221A T_A = +25°C Thermal Resistance, Junction–to–Ambient Thermal Resistance, Junction–to–Case Case 936 (D^2PAK) T_A = +25°C Thermal Resistance, Junction–to–Ambient Thermal Resistance, Junction–to–Case	 P_D θ_{JA} θ_{JC} P_D θ_{JA} θ_{JC}	 Internally Limited 65 5.0 Internally Limited 70 5.0	 W °C/W °C/W W °C/W °C/W
Operating Junction Temperature Range	T_J	–40 to +125	°C
Storage Temperature Range	T_{stg}	–65 to +150	°C

ELECTRICAL CHARACTERISTICS ($V_I–V_O$ = 5.0 V; I_O = 0.5 A for D2T and T packages; T_J = T_{low} to T_{high} [Note 1]; I_{max} and P_{max} [Note 2]; unless otherwise noted.)

Characteristics	Figure	Symbol	Min	Typ	Max	Unit
Line Regulation (Note 3), T_A = +25°C, 3.0 V ≤ $V_I–V_O$ ≤ 40 V	1	Reg_{line}	–	0.01	0.04	%/V
Load Regulation (Note 3), T_A = +25°C, 10 mA ≤ I_O ≤ I_{max} V_O ≤ 5.0 V V_O ≥ 5.0 V	2	Reg_{load}	 – –	 5.0 0.1	 25 0.5	 mV % V_O
Thermal Regulation, T_A = +25°C (Note 6), 20 ms Pulse		Reg_{therm}	–	0.03	0.07	% V_O/W
Adjustment Pin Current	3	I_{Adj}	–	50	100	µA
Adjustment Pin Current Change, 2.5 V ≤ $V_I–V_O$ ≤ 40 V, 10 mA ≤ I_L ≤ I_{max}, P_D ≤ P_{max}	1, 2	ΔI_{Adj}	–	0.2	5.0	µA
Reference Voltage, 3.0 V ≤ $V_I–V_O$ ≤ 40 V, 10 mA ≤ I_O ≤ I_{max}, P_D ≤ P_{max}	3	V_{ref}	1.2	1.25	1.3	V
Line Regulation (Note 3), 3.0 V ≤ $V_I–V_O$ ≤ 40 V	1	Reg_{line}	–	0.02	0.07	% V
Load Regulation (Note 3), 10 mA ≤ I_O ≤ I_{max} V_O ≤ 5.0 V V_O ≥ 5.0 V	2	Reg_{load}	 – –	 20 0.3	 70 1.5	 mV % V_O
Temperature Stability (T_{low} ≤ T_J ≤ T_{high})	3	T_S	–	0.7	–	% V_O
Minimum Load Current to Maintain Regulation ($V_I–V_O$ = 40 V)	3	I_{Lmin}	–	3.5	10	mA
Maximum Output Current $V_I–V_O$ ≤ 15 V, P_D ≤ P_{max}, T Package $V_I–V_O$ = 40 V, P_D ≤ P_{max}, T_A = +25°C, T Package	3	I_{max}	 1.5 0.15	 2.2 0.4	 – –	A
RMS Noise, % of V_O, T_A = +25°C, 10 Hz ≤ f ≤ 10 kHz		N	–	0.003	–	% V_O
Ripple Rejection, V_O = 10 V, f = 120 Hz (Note 4) Without C_{Adj} C_{Adj} = 10 µF	4	RR	 – 66	 65 80	 – –	dB
Long–Term Stability, T_J = T_{high} (Note 5), T_A = +25°C for Endpoint Measurements	3	S	–	0.3	1.0	%/1.0 k Hrs.
Thermal Resistance Junction to Case, T Package		$R_{\theta JC}$	–	5.0	–	°C/W

NOTES:
1. T_{low} to T_{high} = 0° to +125°C, for LM317T, D2T. T_{low} to T_{high} = –40° to +125°C, for LM317BT, BD2T.
2. I_{max} = 1.5 A, P_{max} = 20 W
3. Load and line regulation are specified at constant junction temperature. Changes in V_O due to heating effects must be taken into account separately. Pulse testing with low duty cycle is used.
4. C_{Adj}, when used, is connected between the adjustment pin and ground.
5. Since Long–Term Stability cannot be measured on each device before shipment, this specification is an engineering estimate of average stability from lot to lot.
6. Power dissipation within an IC voltage regulator produces a temperature gradient on the die, affecting individual IC components on the die. These effects can be minimized by proper integrated circuit design and layout techniques. Thermal Regulation is the effect of these temperature gradients on the output voltage and is expressed in percentage of output change per watt of power change in a specified time.

http://onsemi.com
2

Appendix 18: Copy of LM337 Voltage Regulator Data Sheet

ON Semiconductor™

Three-Terminal Adjustable Output Negative Voltage Regulator

The LM337 is an adjustable 3–terminal negative voltage regulator capable of supplying in excess of 1.5 A over an output voltage range of –1.2 V to –37 V. This voltage regulator is exceptionally easy to use and requires only two external resistors to set the output voltage. Further, it employs internal current limiting, thermal shutdown and safe area compensation, making it essentially blow–out proof.

The LM337 serves a wide variety of applications including local, on card regulation. This device can also be used to make a programmable output regulator, or by connecting a fixed resistor between the adjustment and output, the LM337 can be used as a precision current regulator.

- Output Current in Excess of 1.5 A
- Output Adjustable between –1.2 V and –37 V
- Internal Thermal Overload Protection
- Internal Short Circuit Current Limiting Constant with Temperature
- Output Transistor Safe–Area Compensation
- Floating Operation for High Voltage Applications
- Eliminates Stocking many Fixed Voltages
- Available in Surface Mount D^2PAK and Standard 3–Lead Transistor Package

Standard Application

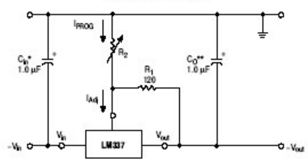

*C_{in} is required if regulator is located more than 4 inches from power supply filter. A 1.0 μF solid tantalum or 10 μF aluminum electrolytic is recommended.

**C_O is necessary for stability. A 1.0 μF solid tantalum or 10 μF aluminum electrolytic is recommended.

$$V_{out} = -1.25\,V\left(1 + \frac{R_2}{R_1}\right)$$

LM337

THREE–TERMINAL ADJUSTABLE NEGATIVE VOLTAGE REGULATOR

SEMICONDUCTOR TECHNICAL DATA

T SUFFIX
PLASTIC PACKAGE
CASE 221A

Heatsink surface connected to Pin 2.

Pin 1. Adjust
2. V_{in}
3. V_{out}

D2T SUFFIX
PLASTIC PACKAGE
CASE 936
(D^2PAK)

Heatsink surface (shown as terminal 4 in case outline drawing) is connected to Pin 2.

ORDERING INFORMATION

Device	Operating Temperature Range	Package
LM337BD2T	T_J = –40° to +125°C	Surface Mount
LM337BT		Insertion Mount
LM337D2T	T_J = 0° to +125°C	Surface Mount
LM337T		Insertion Mount

March, 2001 – Rev. 2

Publication Order Number:
LM337/D

MAXIMUM RATINGS

Rating	Symbol	Value	Unit
Input–Output Voltage Differential	V_I–V_O	40	Vdc
Power Dissipation Case 221A T_A = +25°C Thermal Resistance, Junction–to–Ambient Thermal Resistance, Junction–to–Case Case 936 (D^2PAK) T_A = +25°C Thermal Resistance, Junction–to–Ambient Thermal Resistance, Junction–to–Case	 P_D θ_{JA} θ_{JC} P_D θ_{JA} θ_{JC}	 Internally Limited 65 5.0 Internally Limited 70 5.0	 W °C/W °C/W W °C/W °C/W
Operating Junction Temperature Range	T_J	–40 to +125	°C
Storage Temperature Range	T_{stg}	–65 to +150	°C

ELECTRICAL CHARACTERISTICS ($|V_I–V_O|$ = 5.0 V; I_O = 0.5 A for T package; T_J = T_{low} to T_{high} [Note 1]; I_{max} and P_{max} [Note 2].)

Characteristics	Figure	Symbol	Min	Typ	Max	Unit
Line Regulation (Note 3), T_A = +25°C, 3.0 V ≤ $\|V_I–V_O\|$ ≤ 40 V	1	Reg_{line}	–	0.01	0.04	%/V
Load Regulation (Note 3), T_A = +25°C, 10 mA ≤ I_O ≤ I_{max} $\|V_O\|$ ≤ 5.0 V $\|V_O\|$ ≥ 5.0 V	2	Reg_{load}	 – –	 15 0.3	 50 1.0	 mV % V_O
Thermal Regulation, T_A = +25°C (Note 6), 10 ms Pulse		Reg_{therm}	–	0.003	0.04	% V_O/W
Adjustment Pin Current	3	I_{Adj}	–	65	100	μA
Adjustment Pin Current Change, 2.5 V ≤ $\|V_I–V_O\|$ ≤ 40 V, 10 mA ≤ I_L ≤ I_{max}, P_D ≤ P_{max}, T_A = +25°C	1, 2	ΔI_{Adj}	–	2.0	5.0	μA
Reference Voltage, T_A = +25°C, 3.0 V ≤ $\|V_I–V_O\|$ ≤ 40 V, 10 mA ≤ I_O ≤ I_{max}, P_D ≤ P_{max}, T_J = T_{low} to T_{high}	3	V_{ref}	–1.213 –1.20	–1.250 –1.25	–1.287 –1.30	V
Line Regulation (Note 3), 3.0 V ≤ $\|V_I–V_O\|$ ≤ 40 V	1	Reg_{line}	–	0.02	0.07	%/V
Load Regulation (Note 3), 10 mA ≤ I_O ≤ I_{max} $\|V_O\|$ ≤ 5.0 V $\|V_O\|$ ≥ 5.0 V	2	Reg_{load}	 – –	 20 0.3	 70 1.5	 mV % V_O
Temperature Stability (T_{low} ≤ T_J ≤ T_{high})	3	T_S	–	0.6	–	% V_O
Minimum Load Current to Maintain Regulation ($\|V_I–V_O\|$ ≤ 10 V) ($\|V_I–V_O\|$ ≤ 40 V)	3	I_{Lmin}	 – –	 1.5 2.5	 6.0 10	mA
Maximum Output Current $\|V_I–V_O\|$ ≤ 15 V, P_D ≤ P_{max}, T Package $\|V_I–V_O\|$ ≤ 40 V, P_D ≤ P_{max}, T_J = +25°C, T Package	3	I_{max}	 – –	 1.5 0.15	 2.2 0.4	A
RMS Noise, % of V_O, T_A = +25°C, 10 Hz ≤ f ≤ 10 kHz		N	–	0.003	–	% V_O
Ripple Rejection, V_O = –10 V, f = 120 Hz (Note 4) Without C_{Adj} C_{Adj} = 10 μF	4	RR	 – 66	 60 77	 – –	dB
Long–Term Stability, T_J = T_{high} (Note 5), T_A = +25°C for Endpoint Measurements	3	S	–	0.3	1.0	%/1.0 k Hrs.
Thermal Resistance Junction–to–Case, T Package		$R_{\theta JC}$	–	4.0	–	°C/W

NOTES: 1. T_{low} to T_{high} = 0° to +125°C, for LM337T, D2T. T_{low} to T_{high} = –40° to +125°C, for LM337BT, BD2T.
2. I_{max} = 1.5 A, P_{max} = 20 W
3. Load and line regulation are specified at constant junction temperature. Change in V_O because of heating effects is covered under the Thermal Regulation specification. Pulse testing with a low duty cycle is used.
4. C_{Adj}, when used, is connected between the adjustment pin and ground.
5. Since Long Term Stability cannot be measured on each device before shipment, this specification is an engineering estimate of average stability from lot to lot.
6. Power dissipation within an IC voltage regulator produces a temperature gradient on the die, affecting individual IC components on the die. These effects can be minimized by proper integrated circuit design and layout techniques. Thermal Regulation is the effect of these temperature gradients on the output voltage and is expressed in percentage of output change per watt of power change in a specified time.

References

1. http://www.hiller.org/exhibits/online-exhibits/flying-platform/flying-platform.html *The History of the Hiller Flying Platform*
2. Anselin, A., *The Design and Development of a Flying Platform*, Individual Report, May 2003, University of Exeter
3. Landis, G.A., *Exploring Venus by Solar Airplane*, AIP Conference Proceedings, Vol. 552, 2001, pp.16-18
4. Miura, R., Suzuki, M, *Preliminary Flight Test Program on Telecom and Broadcasting using high altitude platform station*s, Wireless Personal Communications, 24, 341-361, 2003.
5. Frulla, G. *Preliminary Reliability Design of a Solar-Powered High Altitude Very Long Endurance Unmanned Air Vehicle*, Proceedings from the Institute of Mechanical Engineers, Vol.216 Part G: J Aerospace Engineering, 2002, pp.189-196.
6. Tulloch, N.A., *The Design and Development of a Flying Platform*, Individual Report, May 2003, University of Exeter
7. http://www.jmbltd.co.uk/prod_hawker/content_sales_hawker_p01.htm *Hawker 12V 100Ah battery specifications*
8. Gornall, N., *The Design and Development of a Flying Platform*, Individual Report, May 2003, University of Exeter
9. Dushynsky, L., *The Design and Development of a Flying Platform*, Individual Report, May 2004, University of Exeter
10. Mackenzie-Burrows, J.R., *The Design and Development of a Flying Platform*, Minutes, Vol. 1, May 2004, University of Exeter
11. Mackenzie-Burrows, J.R., *The Design and Development of a Flying Platform*, Minutes, Vol. 2, May 2004, University of Exeter
12. Lowis, K., *The Design and Development of a Flying Platform*, Individual Report, May 2004, University of Exeter
13. Holbrook, R.E., *The Design and Development of a Flying Platform*, Individual Report, May 2004, University of Exeter
14. Poczka, C.M.R.A., *The Design and Development of a Flying Platform*, Individual Report, May 2004, University of Exeter
15. Tulloch, N.A., *The Design and Development of a Flying Platform*, Individual Report, May 2003, University of Exeter, p. 56.
16. Mackenzie-Burrows, J.R., *The Design and Development of a Flying Platform*, Minutes, Vol. 1, Meeting 14, May 2004, University of Exeter
17. http://www.batteryuniversity.com/ *Information on all types of rechargeable battery*
18. Data sheet for RS Components product number: 232-6247
19. www.segway.com/segway/component_details.html *Segway Human Transporter technical information*
20. www.saftbatteries.com/140-General/PDF/60-10_news_2002_segway.pdf *Manufacturers of the Segway Human Transporter Batteries*
21. SAFT Ltd, personal correspondence
22. CPC Battery Service, Personal correspondence to Andy
23. Battery Specialists, Personal correspondence via email
24. Batteries Direct, Personal correspondence

25. Tombling, A., *The Design and Development of a Flying Platform*, Individual Report, May 2004, University of Exeter
26. Wright, C.D., *Electromagnetic Wave Propagation*, Course Notes, 2002, University of Exeter
27. Schulze 22-35 Speed Controller Documentation
28. Franco. S., *Electric Circuit Fundamentals,* Saunders College Publishing, 1995, pp 539 – 563.
29. www.windstuffnow.com *Explanation of 3 Phase Systems*
30. Horwood, J.M.K., Personal correspondence
31. Lester, G.A., Personal Correspondence
32. Horowitz, P., Hill, W., *The Art of Electronics*, Cambridge University Press, 2001, pp 113 – 169.